

assay titers can be normalized. Using statistical transformation to better approximate normal distributions and modeling to offset the lack of independence of duplicate assays within an institution, appropriate estimations of the mean titers and confidence intervals have been determined.

Materials and Methods

Reference standard material production

Production and purification of the rAAV2 RSM were carried out at the Vector Core of the University of Florida's Powell Gene Therapy Center between February 2006 and January 2007. The production process has been described in detail elsewhere (Potter *et al.*, 2008) and is briefly summarized here. Production was initiated by cotransfection of HEK293 cells in ten 10-layer Nunc Cell Factories (Thermo Fisher Scientific, Waltham, MA) with plasmid pTR-UF-11, containing the vector genome and eGFP expression cassette (Burger *et al.*, 2004), and the pDG-KanR helper plasmid, a kanamycin-resistant version of pDG (Grimm *et al.*, 1998) at a 1:1 molar ratio, using a calcium phosphate precipitation method. After a 60-hr incubation at 37°C, 5% CO₂, transfected cells were washed with phosphate-buffered saline (PBS) and harvested in PBS containing 5 mM EDTA. Samples of cells were combined with spent tissue culture medium and tested for mycoplasma and *in vitro* adventitious agents. Cells were collected by centrifugation and stored at -20°C until purified. For vector purification, cells were thawed, lysed with 0.5% sodium deoxycholate, treated with Benzonase (Merck, Darmstadt, Germany), and then disrupted by microfluidization. Virions were then purified by STREAMLINE (GE Healthcare Life Sciences, Piscataway, NJ) heparin affinity chromatography. Peak fractions were pooled and applied to a Phenyl Sepharose (GE Healthcare Life Sciences) chromatography column. The flow-through collected from this second purification step was purified and concentrated by sulfopropyl cation-exchange chromatography. Vector was eluted with 5–10 ml of 135 mM NaCl in PBS (equivalent to 285 mM ionic strength) and stored at -80°C. Eighteen batches were prepared and pooled. The purified bulk was diluted to $\sim 2 \times 10^{11}$ vector genomes (VG)/ml with 135 mM NaCl in PBS, and sterile filtered into two 1.3-liter portions. This filtered formulated bulk was stored frozen (-80°C) until vialled. One of the 1.3-liter portions of the bulk was thawed and refiltered, and 0.5 ml was dispensed into 2087 vials at the American Type Culture Collection (ATCC, Manassas, VA) to produce VR-1616, the rAAV2 RSM.

Predistribution testing

Mycoplasma. Mycoplasma testing of the production culture cell harvest and of the filtered formulated bulk purified material was performed at a contract testing laboratory (WuXi AppTec, Shanghai, China). For the cell harvest material, medium and supernatant from each production batch were sampled and pooled for testing. A total of 1×10^7 cells in 15 ml of production culture supernatant was tested according to Good Laboratory Practice (GLP), using the "Points to Consider" assay described by the FDA Center for Biologics Evaluation and Research (CBER/FDA, 1993). This assay detects the presence of mycoplasma by both indirect (cell culture) and direct (broth and agar) assays. The test article

was incubated with monkey kidney cells, stained with a DNA-binding fluorochrome (Hoechst stain), and evaluated microscopically by epifluorescence. Agar and broth flasks were inoculated with test article and incubated anaerobically and aerobically, respectively. Broths were subcultured onto agar plates on days 3, 7, and 14 days postinoculation. All plates were examined no sooner than 14 days postinoculation. Purified bulk rAAV2 RSM was tested by a modification of the "Points to Consider" assay, in which three cycles of inoculation and incubation on Vero cells precede the assay to allow amplification of mycoplasma. Both harvested material and purified bulk material were also tested, using a PCR assay directed against the 16S rRNA gene of various mycoplasma species (WuXi AppTec).

Bioburden. The presence of aerobes, fungi, spores, and anaerobes in the purified bulk material was quantified by plating on various media under specific incubation conditions (WuXi AppTec). The sensitivity of this assay is <5 colony-forming units (CFU)/ml.

Sterility. The vialled rAAV2 RSM (cat. no. VR-1616; ATCC) was tested for sterility at the Indiana University Vector Production Facility (Indianapolis, IN) according to GLP guidelines. The presence of aerobes, anaerobes, and fungi was tested by direct inoculation of thioglycolate broth, Trypticase soy broth, and Sabouraud dextrose agar and incubation for 14 days at the appropriate temperature. Negative and positive (*Bacillus subtilis*, *Candida albicans*, and *Bacteroides vulgatus*) controls were included.

Endotoxin. The vialled rAAV2 RSM was also tested for endotoxin at the Indiana University Vector Production Facility according to GLP guidelines and using the *Limulus* ameocyte lysate gel-clotting assay. Test samples were assayed in duplicate and diluted 2-fold with water. The test reagent (100 μ l) was added to the rAAV2 RSM dilution and incubated at 37°C for 60 min, and the tube was examined for the presence of a gel clot. Negative, positive, and spiked controls were included. The sensitivity of the assay was 0.06 endotoxin unit (EU)/ml.

Prevailing stability study. An rAAV2-GFP vector preparation at 2×10^{11} VG/ml, in the same formulation as the rAAV2 RSM (PBS + 135 mM NaCl), was placed in polypropylene and glass vials (not siliconized) at 0.5 ml per vial. Vials of each type were stored at both temperatures. Vials held at room temperature were assayed for infectious titer after 1 hr, 1 day, 3 days, and 7 days; vials stored at -80°C were assayed for infectious titer at 1 hr, 1 day, 14 days, 35 days, and 124 days (Potter *et al.*, 2008).

RSM handling stability study. The rAAV2 RSM was thawed on ice and aliquoted into siliconized plastic vials. Aliquots were either tested immediately for transducing titer, infectious titer, and vector genome titer or stored at 4°C or -80°C for 3 days and then tested.

rAAV2 RSM handling. For AAV2 RSM characterization, each testing laboratory received two vials from the ATCC on dry ice. On receipt both vials were stored frozen at -70°C to -90°C. One vial was thawed at room temperature while

mixing gently and then kept on wet ice. Within 1 hr of thawing, the infectious titer and transducing titer assays were conducted. The remainder of the thawed vial was stored at 4°C and mixed gently on use. Within 5 days of vial thaw, the particle titer, vector genome titer, and purity/identity assays were performed. These steps were repeated for the second vial, starting on a different calendar day.

rAAV2 RSM characterization assays

Brief descriptions of each characterization assay follow. For those wishing to reproduce these assays, detailed protocols can be found at the links specified below or may be requested directly from M. Lock or R. Snyder.

Particle titer. Particle concentration was determined by each laboratory, using four separate dilution series from a single vial in the Progen AAV2 titration ELISA (cat. no. PRATV; Progen Biotechnik), by comparison with a standard curve prepared from a previously titered rAAV2 preparation. See the protocol posted at http://www.isbiotech.org/ReferenceMaterials/pdfs/AAV2_capsid_titer_assay_V2.pdf

Vector genome titer. Vector genome concentration was determined in duplicate, testing one replicate from each of two vials, by quantitative PCR of serial dilutions of rAAV2 RSM against a standard curve of plasmid pTR-UF-11 (MBA-331; ATCC) (Burger *et al.*, 2004) See the protocol posted at http://www.isbiotech.org/ReferenceMaterials/pdfs/AAV2_RSS_genome_copy_titration_QPCR.pdf

Transducing titer. Serial 10-fold dilutions of rAAV2 RSM were made on HeLaRC32 cells (CRL-2972; ATCC) (Chadeuf *et al.*, 2000) and coinfecting with adenovirus type 5 (VR-1516; ATCC). Fluorescence microscopy was used to count GFP-expressing cells at 72 hr postinfection. See the protocol posted at http://www.isbiotech.org/ReferenceMaterials/pdfs/AAV2_RSS_infectious_titer_assays_V2.pdf

Infectious titer. Serial 10-fold dilutions of an rAAV2 reference standard stock (RSS) were made on HeLaRC32 cells (CRL-2972; ATCC) and coinfecting with adenovirus type 5 (VR-1516; ATCC). Seventy-two hours postinfection total cell DNA was extracted and analyzed for vector genome copies by qPCR. Input vector genomes were subtracted and TCID₅₀ titers were calculated according to the method of Kärber (Kärber, 1931). See the protocol posted at http://www.isbiotech.org/ReferenceMaterials/pdfs/AAV2_RSS_infectious_titer_assays_V2.pdf

Purity and identity. The purity and identity of the rAAV2 RSM were evaluated by SDS-PAGE, using SYPRO ruby (Invitrogen, Carlsbad, CA) or silver staining (SilverXpress; Invitrogen). The AAV2 VP1, VP2, and VP3 capsid protein bands were evaluated for their stoichiometry and size. Purity relative to nonvector impurities visible on stained gels was determined. Vector identity was verified by observation of the electrophoretic banding pattern expected for AAV2 and by comparison with positive controls. See the protocol posted at http://www.isbiotech.org/ReferenceMaterials/pdfs/AAV2_RSS_identity-purity_assay.pdf

Results

rAAV2 RSM production and predistribution testing

The goal of the AAV2RSWG manufacturing subcommittee was to make a single lot of an rAAV-eGFP vector with a yield of 1×10^{15} vector genomes. Eighteen batches of ten 10-layer cell factories containing 293 cells were transfected and the resulting AAV vector was purified from the transfected cells by sequential heparin affinity, hydrophobic interaction, and cation-exchange chromatography. The final column eluates from the 18 batches prepared were pooled for a total of 150 ml. The genome titer of this purified bulk was assayed by dot-blot assay and, using this method, it was determined that the material contained 5.69×10^{14} VG (Potter *et al.*, 2008). The purified bulks were combined, diluted to $\sim 2 \times 10^{11}$ VG/ml, and sterile filtered into two 1.3-liter portions. This filtered formulated bulk was stored frozen (-80°C) in anticipation of vialing. In March 2008, one of the 1.3-liter portions of the bulk stock was thawed, refiltered, and dispensed into 2087 vials at the ATCC to produce the rAAV2 RSM (cat. no. VR-1616). The vials, frozen in the repository at the ATCC, are available for distribution. The other 1.3-liter portion of the bulk material remains frozen at the ATCC, to be dispensed at a later date if demand warrants (Potter *et al.*, 2008).

Before freezing, the filtered formulated bulk was sampled (5 ml) and tested for bioburden by a contract testing laboratory (WuXi AppTec). Aerobes, fungi, spores, and obligate anaerobes all tested negative with an assay sensitivity of <5 CFU/sample. Before distribution, the vialled rAAV2 RSM was tested under GLP guidelines for sterility (aerobes, anaerobes, fungi) and endotoxin at the Indiana University Vector Production Facility. No bacterial or fungal contamination was detected and endotoxin levels were less than 0.06 EU/ml. The production culture cell harvest and the filtered purified bulk material were tested at WuXi AppTec for mycoplasma contamination as detailed in Materials and Methods (GLP "Points to Consider" assay). The harvest material tested positive for *Mycoplasma arginini* (bovine origin) and the tests were valid (i.e., all controls performed). The filtered purified bulk material was tested for mycoplasma, using a modified assay with increased sensitivity. In this test, a sample of the bulk material was passaged three times on Vero cells before performing the GLP "Points to Consider" assay. The bulk material tested negative for mycoplasma whereas the spike-in controls performed as expected, indicating that the assay was valid. Last, the harvest and bulk materials were tested by PCR (WuXi AppTec) for a 16S rRNA gene region specific to various mycoplasma species. Using this assay, the harvest was confirmed positive and the filtered formulated bulk again tested negative, with all controls performing as expected. Thus whereas the harvested cells were positive for mycoplasma, the purified bulk was negative for viable mycoplasma and no mycoplasma DNA was detected, so it was concluded that the purification process likely separated and/or inactivated the contaminating mycoplasma present in the harvest material (Potter *et al.*, 2008).

Beta testing

The AAV2RSWG Quality Control subcommittee was formed for the purpose of characterizing the rAAV2 RSM.

TABLE 1. rAAV2 REFERENCE STANDARD MATERIAL TESTING LABORATORIES

University of Naples Federico II, Italy
University of North Carolina Vector Laboratories, USA
Universitat Autònoma de Barcelona, Spain
Research Institute at Nationwide Children's Hospital, USA
University of Florida, USA
Laboratoire de Thérapie Génique, France
Généthon, France
Applied Genetic Technologies, USA
International Center for Genetic Engineering and Biotechnology (ICGEB), Italy
German Cancer Research Center (DKFZ), Germany
University of Pennsylvania, USA
Jichi Medical University, Japan
Sangamo BioSciences, USA
Université Libre de Bruxelles, Belgium
Amsterdam Molecular Therapeutics, The Netherlands
Children's Hospital of Philadelphia, USA

Decisions regarding the characterization assays required were made in consultation with the AAV2RSWG, and members were invited to submit their assay protocols. These protocols were reviewed and a lead protocol was chosen for each assay. The assays chosen included (1) confirmation of the serotype and capsid particle titer by A20 ELISA (Progen Biotechnik); (2) determination of vector genome titer by qPCR; (3) determination of infectious titer by median tissue culture infective dose (TCID₅₀) with qPCR readout and by transduction (GFP readout); (4) evaluation of the purity, capsid subunit stoichiometry, and chemical integrity of the capsid by SDS-PAGE.

During the protocol selection process it was realized that the highest level of assay reproducibility in the various testing laboratories could be ensured only if certain reagents were provided along with the rAAV2 RSM. The reagents, which are now available from the ATCC, include a cell line expressing the AAV2 *rep* and *cap* genes (HeLa32; kindly provided by P. Moullier, INSERM UMR649 Nantes, France), a concentrated adenovirus helper virus (the adenovirus type 5 reference standard material, ARM) (VR-1516; ATCC) for the transduction and infectivity assays, and the pTR-UF-11 vector plasmid (kindly provided by S. Zolotukhin, Powell Gene Therapy Center and Division of Cellular and Molecular Therapy, Department of Pediatrics, University of Florida, Gainesville, FL) used to manufacture the AAV2 RSM viral

vector. For both genome titer and infectious titer assays, a qPCR primer-probe set directed to the simian virus 40 (SV40) poly(A) sequence and a dilution series specific to the RSM were selected. For the purity and identity assay, commercially available assay reagents with the highest sensitivity were suggested. Using these reagents, the modified assay protocols were beta tested at the University of Pennsylvania Gene Therapy Program against both in-house standards (AAV2.CMV.eGFP and AAV2.CMV.lacZ) and the rAAV2 RSM itself. The genome, infectious, and transduction titers of the in-house standards correlated well with the titers previously established by in-house assays (see Table 2; and data not shown) and vector genome-to-infectious or transduction unit ratios were similar to those published elsewhere (Salvetti *et al.*, 1998; Zolotukhin *et al.*, 1999; Zen *et al.*, 2004). Repeating the beta testing with the rAAV2 RSM allowed appropriate dilution ranges to be established for several of the characterization assays. The finalized protocols were posted at the International Society for BioProcess Technology website (www.ISBioTech.org) and the HeLaRC32 cells (CRL-2972; ATCC), pTR-UF-11 plasmid (MBA-331; ATCC), and ARM (VR-1516; ATCC) assay reagents were made available through the ATCC. The rAAV2 RSM (VR-1616; ATCC) was distributed along with the required reagents and handling instructions to 16 laboratories worldwide (Table 1) that volunteered to conduct one or more of the characterization assays.

Before filling the rAAV2 RSM, a study was conducted with a different lot of rAAV2-GFP vector in the same formulation to evaluate the short-term stability of the vector at room temperature (the filling condition) and at -80°C (the storage condition). Vials were filled with the beta test vector and held at the test temperatures for the time periods indicated (see Materials and Methods) and were then assayed for infectious titer. In all scenarios, a 30–40% drop was observed between the initial titer and the average of all samples taken during the time course and it was assumed that this loss likely indicated absorption to the container surfaces at the low vector concentration (Potter *et al.*, 2008), because these containers were not silicized. After filling the rAAV2 RSM, a limited study was also conducted to evaluate the stability of the rAAV2 RSM after post-thaw storage at 4°C , and after refreezing at -80°C . The purpose of the study was to determine the appropriate conditions for handling of the RSM once received by the testing laboratory. Transduction titers fell 35 and 56% after storage or refreezing at 4°C and -80°C , respectively, and infectious titer fell 78 and 63%, respectively

TABLE 2. QUALIFICATION OF REFERENCE STANDARD MATERIAL (RSM) TESTING METHODS USING IN-HOUSE STANDARDS AND BETA TESTING OF rAAV2 RSM UNDER VARIOUS STORAGE CONDITIONS

	In-house standards		rAAV2 RSM		
	AAV2.CMV.e.GFP	AAV2.CB.lacZ	At thaw	4°C^a	-80°C^a
Transducing titer (GFU/ml)	1.42×10^{10}	NA	1.89×10^9	1.23×10^9	8.38×10^8
Infectious titer (TCID ₅₀ IU/ml)	6.96×10^{10}	2.42×10^{11}	1.65×10^{10}	3.56×10^9	6.23×10^9
Physical titer (vector genomes/ml)	4.53×10^{12}	2.15×10^{12}	3.39×10^{10}	3.39×10^{10}	3.41×10^{10}
Vector genomes: infectious units	65	8.87	2.05	9.53	5.39
Vector genomes: transducing units	319	NA	17.90	27.50	40.70

Abbreviations: GFU, GFP (green fluorescent protein) forming units; NA, not available; TCID₅₀, median tissue culture infective dose.

^a Assayed 3 days postthawing, after storage at the indicated temperature.

(Table 2). Conversely, no change was observed in the vector genome titers under the various storage conditions. These results indicated that the postthaw storage conditions were adversely affecting the potency of the rAAV2 RSM and that this decrease was not due to absorption to the siliconized aliquot vials used in this study, because the vector genome titer was unchanged. On the basis of these data the decision was made to test two separate aliquots of the RSM and to determine transducing and infectious titers within 1 hr of thawing a vial.

rAAV2 RSM characterization

The characterization phase of the rAAV2 RSM proceeded from July 2008 to March 2009. On receipt, the RSM was evaluated by the 16 testing laboratories according to the

posted protocols, and data were recorded on the assay worksheets provided, which contained the necessary calculations for titer determination. Fifteen laboratories performed the particle titer assay (31 replicates), 16 laboratories performed the genome titer assay (36 replicates), 10 laboratories performed the infectious titer assay (23 replicates), and 12 laboratories performed the transducing titer assay (19 replicates). In some cases (four of the tests), substantial experimental deviation from the posted protocols was noted and these data have been omitted from the statistical analyses.

The raw data that emerged from the testing laboratories for the four quantitative titer assays (Table 3) was statistically analyzed to determine true mean titer values and confidence intervals. The distribution was first visualized as histograms (Fig. 1), and it was noted that with the possible exception of the particle titer results, the data do not appear to be nor-

TABLE 3. rAAV2 REFERENCE STANDARD MATERIAL RAW CHARACTERIZATION DATA

Laboratory	Replicate	Particle titer (ELISA) (pt/ml)	Genome titer (qPCR) (VG/ml)	Transducing titer (green cells) (GFU/ml)	Infectious titer (TCID ₅₀) (IU/ml) ^a
A	1	1.08 × 10 ¹²	4.68 × 10 ¹⁰	1.27 × 10 ⁹	
	2	1.26 × 10 ¹²	8.77 × 10 ¹⁰	1.26 × 10 ⁹	
B	1	8.25 × 10 ¹¹	7.03 × 10 ¹⁰	3.63 × 10 ⁸	6.32 × 10 ⁹
	2	8.28 × 10 ¹¹	7.58 × 10 ¹⁰	1.00 × 10 ⁸	1.36 × 10 ⁹
	3		9.39 × 10 ¹⁰	7.15 × 10 ⁷	2.00 × 10 ⁹
C	1	7.70 × 10 ¹¹	8.60 × 10 ¹⁰	9.80 × 10 ⁶	
	2	6.05 × 10 ¹¹	4.19 × 10 ¹⁰		
D	1	8.80 × 10 ¹¹	1.01 × 10 ¹⁰	1.70 × 10 ⁹	1.02 × 10 ¹⁰
	2	7.83 × 10 ¹¹	3.71 × 10 ¹⁰	2.77 × 10 ⁹	6.96 × 10 ⁹
E	1	1.16 × 10 ¹²	1.58 × 10 ¹⁰		
	2	1.04 × 10 ¹²	1.14 × 10 ¹⁰		
	3		1.61 × 10 ¹⁰		
F	1	1.66 × 10 ¹²	2.17 × 10 ¹⁰	6.60 × 10 ⁸	
	2	1.01 × 10 ¹²	2.12 × 10 ¹⁰	5.70 × 10 ⁸	
G	1	1.90 × 10 ¹²	1.13 × 10 ¹⁰	4.02 × 10 ⁸	3.23 × 10 ⁹
	2	9.39 × 10 ¹¹	1.30 × 10 ¹⁰		2.67 × 10 ⁹
H	1		2.04 × 10 ¹⁰		
	2		2.13 × 10 ¹⁰		
I	1	8.56 × 10 ¹¹	5.93 × 10 ¹⁰	2.20 × 10 ⁷	
	2	7.08 × 10 ¹¹	6.10 × 10 ¹⁰	2.95 × 10 ⁷	
J	1	1.24 × 10 ¹²	3.39 × 10 ¹⁰	1.89 × 10 ⁹	1.65 × 10 ¹⁰
	2	1.07 × 10 ¹²	4.49 × 10 ¹⁰	1.22 × 10 ⁹	2.42 × 10 ¹⁰
K	1	5.29 × 10 ¹¹	3.72 × 10 ¹⁰	2.01 × 10 ⁸	
	2	7.75 × 10 ¹¹	3.62 × 10 ¹⁰	2.04 × 10 ⁸	
L	1	8.13 × 10 ¹¹	1.31 × 10 ⁹	5.96 × 10 ⁸	1.50 × 10 ⁹
	2	4.99 × 10 ¹¹	1.63 × 10 ¹⁰	6.48 × 10 ⁸	6.96 × 10 ⁸
M	1	1.11 × 10 ¹¹	1.16 × 10 ¹⁰	8.88 × 10 ⁸	2.00 × 10 ⁹
	2	1.25 × 10 ¹¹	1.53 × 10 ¹⁰	4.52 × 10 ⁸	1.50 × 10 ⁹
N	1	3.93 × 10 ¹¹	1.47 × 10 ¹⁰	3.82 × 10 ⁸	2.00 × 10 ¹⁰
	2	5.59 × 10 ¹¹	7.63 × 10 ⁹	2.62 × 10 ⁸	7.66 × 10 ⁹
	3	9.58 × 10 ¹¹	4.24 × 10 ⁹		2.40 × 10 ⁹
O	1	1.06 × 10 ¹²	6.04 × 10 ¹⁰		
	2	1.09 × 10 ¹²	1.27 × 10 ¹¹		
P	1	8.02 × 10 ¹¹	4.20 × 10 ¹⁰		7.66 × 10 ⁹
	2	7.74 × 10 ¹¹	5.10 × 10 ¹⁰		6.96 × 10 ⁹
	3		4.82 × 10 ¹⁰		9.28 × 10 ⁹
Mean		9.43 × 10 ¹¹	3.82 × 10 ¹⁰	6.94 × 10 ⁸	7.00 × 10 ⁹
Standard deviation		3.19 × 10 ¹¹	2.97 × 10 ¹⁰	7.03 × 10 ⁸	6.70 × 10 ⁹

^aFour replicate test results were omitted because of documented experimental deviation from the posted protocols.

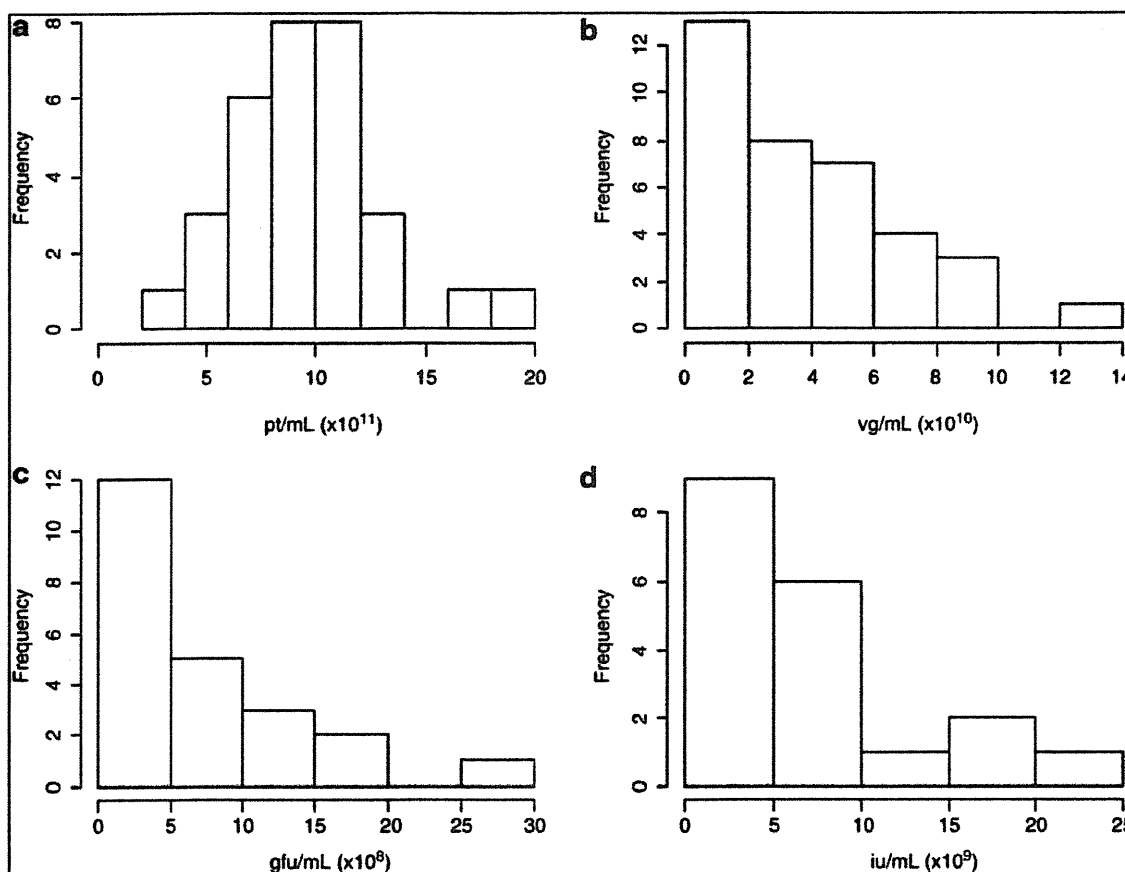


FIG. 1. Histograms displaying the distributions of (a) particle titer (pt/ml), (b) vector genome titer (VG/ml), (c) transducing titer (GFU/ml), and (d) infectious titer (IU/ml).

mally distributed. Because valid estimation of the mean and confidence interval relies on an underlying normal distribution, it was clear that some form of transformation was warranted. Common statistical transformation methods employed are square root, natural log, and log base 10. Means and intervals are calculated on the transformed data and the results are then back-transformed to the original measurement scale; the data for each assay were processed in this way, using all three transformations. Analysis of the mean and median (for normally distributed data these two values are the same) and skewness and kurtosis estimates confirmed that the transformations were performing as expected (data not shown). Figure 2 shows the results of the most successful transformations for each assay as quantile-quantile plots. In this analysis the quantiles (i.e., 5%, 10%, etc.) obtained from the transformed data are compared with the quantiles that would be expected for a normal distribution. A line that extends through the 25th and 75th quantile is shown on the plots and the nearer the points are to this line, the more normal the data distribution. With the exception of two extreme points, the capsid particle titer assay data appeared normally distributed without the need for transformation. For the vector genome titer and the transduction titer, square root transformation appeared to approximate normal distribution and seemed warranted. For the infectious titer, a log base 10 transformation appeared the

most appropriate. The transformed data are summarized in Table 4. For each assay, 2 and 3 standard deviation limits were calculated corresponding to nominal 95 and 99.7% confidence bounds on individual values. Any test result lying outside of the 3 standard deviations was considered to be an outlier. Using this criterion only a single test result (from the particle titer assay) was determined to be an outlier and was removed from the analysis; the values reported in Table 4 exclude this data point.

An assumption we have made when calculating the mean values and confidence intervals is that each test result is independent of another; however, this assumption does not take into account that all institutions submitted duplicate (and in some cases triplicate) test results for the assays. To assess the degree of correlation between the two duplicate samples, Pearson coefficients were determined. These estimates ranged from 0.57 to 0.84 for the four assays (where a value of 1 indicates a perfect correlation). The results indicate that there is a significant correlation within institution and that the assumption that each result is independent is violated. To account for this correlation, the transformed data were modeled, using a linear random effect modeling approach (Littell *et al.*, 2006). This allows for a unique component associated with each institution to be included in the model, under the assumption that these institutional random effects have a mean of zero. When the correlation within an

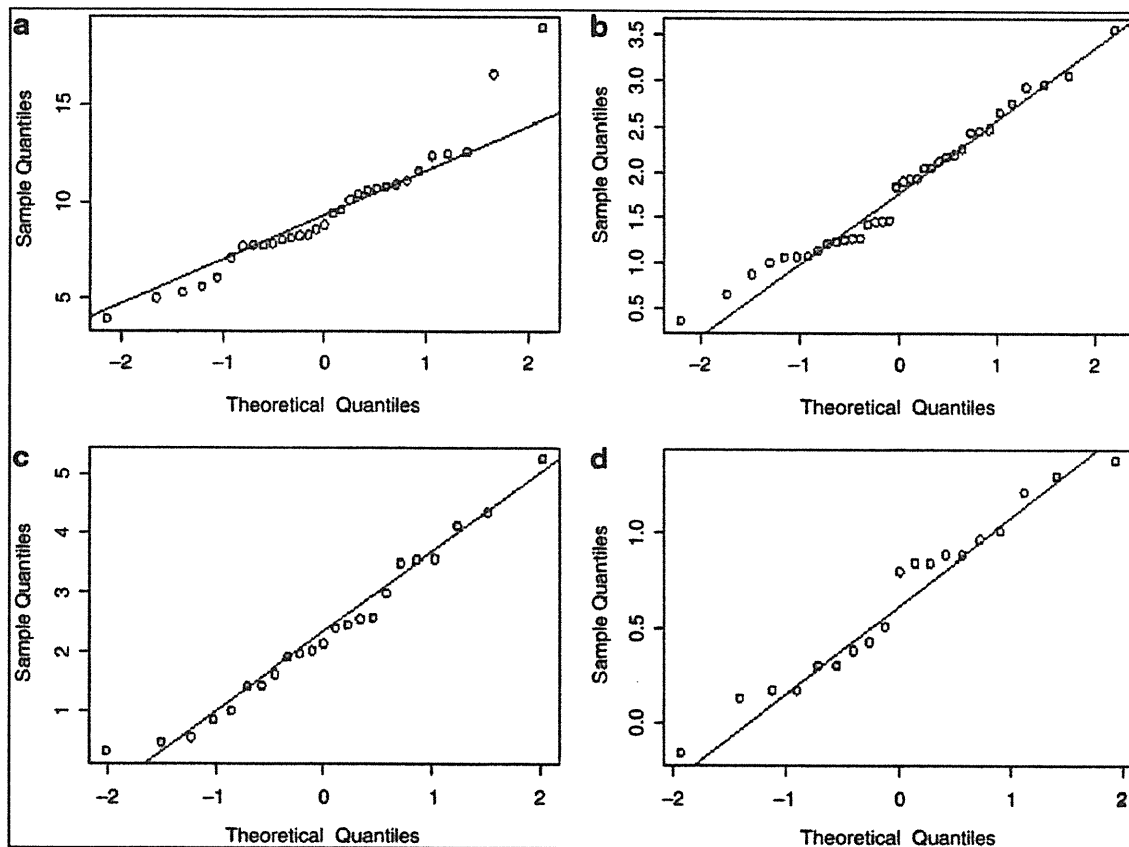


FIG. 2. Quantile-quantile plots displaying sample versus normal quantiles of (a) particles per milliliter, (b) square root of vector genomes per milliliter, (c) square root of transducing units per milliliter, and (d) \log_{10} infectious units per milliliter. Lines pass through the 25th and 75th quantiles.

institution is accounted for, the precision of the mean estimate as illustrated by the width of the 95% confidence interval is decreased (Table 5). Taking the transformed, modeled data as the true estimate of the mean, we have arrived at the following determinations for the rAAV2 RSM: the mean particle titer is 9.18×10^{11} particles/ml with 95% confidence that the true value lies in the range of 7.89×10^{11}

to 1.05×10^{12} particles/ml; the mean vector genome titer is 3.28×10^{10} vector genomes/ml with 95% confidence that the true value lies in the range of 2.70×10^{10} to 4.75×10^{10} vector genomes/ml; the mean transducing titer is 5.09×10^8 transducing units/ml with 95% confidence that the true value lies in the range of 2.00×10^8 to 9.60×10^8 transducing units/ml; and the mean infectious titer is 4.37×10^9 TCID₅₀ IU/ml with

TABLE 4. rAAV2 REFERENCE STANDARD MATERIAL TITER ESTIMATES AFTER TRANSFORMATION

Titer units (method)	Transformation ^a	Mean	Lower 95% confidence limit for the mean	Upper 95% confidence limit for the mean	± 2 SD	± 3 SD
Particles/ml (ELISA)	Untransformed	9.11×10^{11}	8.10×10^{11}	1.01×10^{12}	3.73×10^{11} – 1.45×10^{12}	1.04×10^{11} – 1.78×10^{12}
Vector genomes/ml (qPCR)	Square root	3.26×10^{10}	2.41×10^{10}	4.25×10^{10}	8.82×10^8 – 1.10×10^{11}	0 – 1.66×10^{11}
Transducing units/ml (green cells)	Square root	5.29×10^8	2.99×10^8	8.23×10^8	0 – 2.43×10^9	0 – 3.90×10^9
Infectious units/ml (TCID ₅₀)	Log ₁₀	4.49×10^9	2.75×10^9	7.29×10^9	5.94×10^8 – 3.39×10^{10}	2.16×10^8 – 9.31×10^{10}

^aUsed to better qualify the assumption of normal distribution for the purpose of determining distributional values.

TABLE 5. FINAL rAAV2 REFERENCE STANDARD MATERIAL TITER ESTIMATES AFTER TRANSFORMATION AND MODELING

Titer units (method)	Transformation ^a	Mean	Lower 95% confidence limit for the mean	Upper 95% confidence limit for the mean	± 2 SD	± 3 SD
Particles/ml (ELISA)	Untransformed	9.18 × 10 ¹¹	7.89 × 10 ¹¹	1.05 × 10 ¹²	3.73 × 10 ¹¹ –1.45 × 10 ¹²	1.04 × 10 ¹¹ –1.78 × 10 ¹²
Vector genomes/ml (qPCR)	Square root	3.28 × 10 ¹⁰	2.70 × 10 ¹⁰	4.75 × 10 ¹⁰	9.00 × 10 ⁸ –1.04 × 10 ¹¹	0–1.66 × 10 ¹¹
Transducing units/ml (green cells)	Square root	5.09 × 10 ⁸	2.00 × 10 ⁸	9.60 × 10 ⁸	0–2.47 × 10 ⁹	0–4.00 × 10 ⁹
Infectious units/ml (TCID ₅₀)	Log ₁₀	4.37 × 10 ⁹	2.06 × 10 ⁹	9.26 × 10 ⁹	5.15 × 10 ⁸ –3.71 × 10 ¹⁰	1.77 × 10 ⁸ –1.08 × 10 ¹¹

^aUsed to better qualify the assumption of normal distribution for the purpose of determining distributional values.

95% confidence that the true value lies in the range of 2.06 × 10⁹ to 9.26 × 10⁹ TCID₅₀ IU/ml. The mean vector genome titer of 3.28 × 10¹⁰ VG/ml is almost 1 log lower than the titer of 2 × 10¹¹ VG/ml assessed for the diluted purified bulk harvest before vialing. The discrepancy between the bulk material and final fill may be due to loss of vector after filtering of the bulk product, to the different assay methods used for the titering (dot-blot vs. qPCR), or a combination of both. The bulk vector was titered at the University of Florida, using the method of dot-blot hybridization to determine the appropriate formulation volume for the final fill. It is possible that the loss, if any, occurred during the final filtration and filling of the dilute reference standard material at the ATCC (diluted nearly 1000 times relative to preparations that are used preclinically or clinically). The product that was vialled and frozen constitutes the reference standard material that was characterized, and that is available to the community.

Some important properties of the rAAV2 RSM are indicated by the ratios of the titers (Table 6). The vector genome-to-infectious titer (VG:IU) ratio is often used as a measure of the relative infectivity of the vector, with lower ratios reflecting more infectious preparations. The rAAV2 RSM VG:IU ratio is 7.5, which indicates that the RSM has retained infectivity. The vector genome-to-transduction titer (VG:TU) ratio is 8.6-fold higher than the VG:IU ratio, and this result reflects the different sensitivities of the infectivity and transduction (measuring infectivity and gene expression) assays. Another ratio that is often used is the particle-to-vector genome titer ratio (P:VG). This ratio indicates the ratio of total particles, including both empty and full, to those particles containing the vector genome. The P:VG ratio obtained for the rAAV2 RSM is 28 and indicates a large excess of empty particles. This finding is consistent with the fact that the chromatographic purification process used in the production of the rAAV2 RSM was not designed to separate

empty and full particles. One concern is that empty particles may have adversely affected the performance of the rAAV2 RSM in transduction and infectivity assays. However, during beta testing, two triple-transfected CsCl-purified lots (one each of AAV2.CMV.eGFP and AAV2.CMV.lacZ) were tested, using the RSS characterization methods: vector genome (qPCR), TCID₅₀, and where applicable eGFP transduction titering. Because these were CsCl-purified preparations the empty capsid content is lower than in preparations purified by chromatography. The VG:TCID₅₀ IU ratios and VG:TU ratios were similar or greater than those obtained for the reference standard (Tables 2 and 6). Similarly, the VG:TCID₅₀ IU ratios and VG:TU ratios of the reference standard (Table 6) are similar to those reported in the literature for other AAV2 vectors (Salvetti *et al.*, 1998; Zolotukhin *et al.*, 1999; Zen *et al.*, 2004).

The purity of the rAAV2 RSM was assessed and the capsid identity confirmed by SDS-PAGE analysis. The RSM was examined under both reducing and nonreducing conditions, using SYPRO ruby and silver stains (Fig. 3). Under reducing conditions all proteins including the denatured AAV2 capsids are expected to enter the gel and impurities would be detected as protein bands other than the capsid proteins VP1, VP2, and VP3. Under nonreducing conditions the capsid would remain intact and would not be expected to enter the resolving gel, whereas impurities would enter the gel; proteins that previously comigrated with the capsid proteins on reducing gels would thus be detected. Silver nitrate staining was included because it is capable of detecting DNA, lipid, and carbohydrate impurities as well as nanogram levels of protein (Weiss *et al.*, 2009). SYPRO ruby is a protein-specific fluorescent dye that has a sensitivity close to that of silver stain (Rabilloud *et al.*, 2001; Weiss *et al.*, 2009). In each case the rAAV2 RSM was analyzed alongside an internal laboratory standard AAV2 vector. The consensus data from the 11 testing laboratories that carried out the purity/identity test estimated that the rAAV2 RSM was greater than 94% pure and confirmed that VP1, VP2, and VP3 comigrated with the AAV2 capsid proteins of the internal vector standards (Fig. 3; and data not shown).

Discussion

As rAAV vectors more frequently head toward the clinic for gene therapy trials, there is an increasing need to share pharmacokinetic, toxicologic, and efficacy data. This need is

TABLE 6. rAAV2 REFERENCE STANDARD MATERIAL TITER RATIOS

	Ratio
Particles: vector genomes ^a	27.99
Vector genomes: infectious units	7.51
Vector genomes: transducing units	64.44
Particles: infectious units	210.07

^aA measure of the ratio of total particles to full particles.

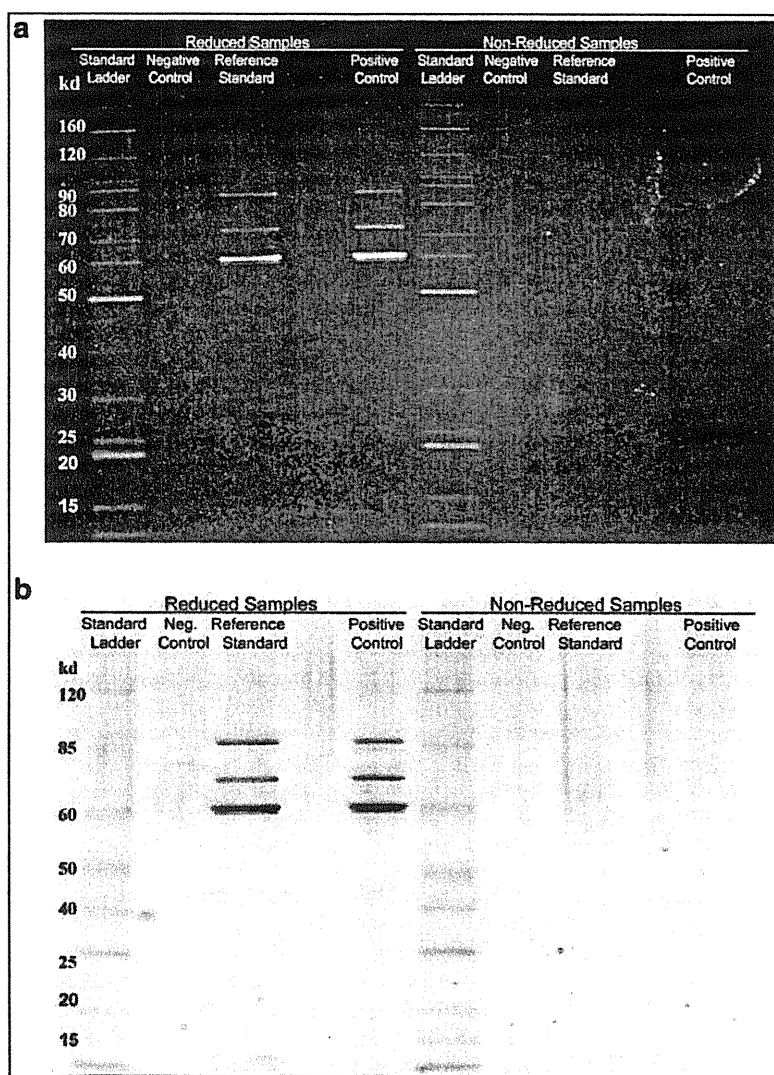


FIG. 3. The rAAV2 RSM was run on SDS-polyacrylamide gels under both reducing and native conditions and then stained with (a) SYPRO ruby or (b) silver stain. An in-house rAAV2 standard was run as a positive control and buffer as a negative control. The lanes for each gel are as follows: (1) benchmark ladder (unstained or prestained)—reduced; (2) negative control—reduced; (3) AAV reference material—reduced; (5) positive control—reduced; (6) benchmark ladder (unstained or prestained)—native; (7) negative control—native; (8) AAV reference material—native; (10) positive control—native.

currently confounded by the lack of standardization of critical vector parameters such as vector strength and potency. The standardization issues arise because different assays or different protocols for the same assay are often used by individual investigators to measure an identical vector property. The introduction of a widely accepted rAAV reference standard would allow laboratories to characterize AAV vectors in terms of common units, therefore facilitating comparison of doses determined by disparate assays and permitting safe and effective dosage at equivalent levels. Furthermore, efficacy and toxicology data reported in the literature could be used as a guide for initial dosing in animals and humans.

Here we have described the characterization of the first rAAV reference standard, an AAV serotype 2 vector. The goal of the AAV2RSWG was to provide a stable, high-quality, highly characterized RSM that would be both accepted and easily accessed by the AAV research community. As pointed out by FDA officials at the beginning of the effort, a reference standard material does not need to be pure or the

“best,” it just needs to be well characterized. Furthermore, there are many examples of viral reference standard materials from the World Health Organization (WHO, Geneva, Switzerland) and the National Institute for Biological Standards and Control (NIBSC, Potters Bar, UK) that are not pure (e.g., poliovirus and hepatitis B virus references). Although the rAAV2 RSM was made in a research vector core and not at a current Good Manufacturing Procedure (cGMP) facility, it was extensively tested for adventitious agents and contaminants. The final rAAV2 RSM product was negative for adventitious agents in all tests to which it was subjected, although the harvest material was exposed to mycoplasma that was cleared and/or inactivated in the purification process, because the purified bulk tested negative for viable mycoplasma and mycoplasma DNA (Potter *et al.*, 2008). Because the rAAV2 RSM is a reference standard to be used in research and quality control (QC) laboratories and is not intended for use in humans, the AAV2RSWG recommended that filling, banking, and characterization proceed. A summary of the mycoplasma testing will be included on the

product information sheet supplied with each shipment of the rAAV2 RSM, stating that the reference standard has been exposed to mycoplasma, but is mycoplasma-free. Thus, institutions and companies requesting the rAAV2 RSM will be fully informed and can decide if they want to bring it into their QC laboratories. The reference material is intended to be restricted to QC laboratories, isolated from production suites. In addition, it is envisioned that internal reference standards will be calibrated against the AAV2 RSM one time and then used on a routine basis for product-specific testing.

The short-term stability testing performed on the surrogate AAV2-GFP vector as well as on the final vial of rAAV2 RSM material suggested that some loss of vector potency was occurring on storage. Initially this loss was assumed to be due to adsorption to the surfaces of the vial as was seen in the previous study using vials that were not siliconized (Potter *et al.*, 2008); however, when vector genomes were assayed no corresponding loss was seen when using siliconized vials (Table 2). One explanation for the loss of potency observed may be the omission of a stabilizing excipient in the final formulation (Croyle *et al.*, 2001; Wright *et al.*, 2003). The beta test stability results influenced the way the rAAV2 RSM was handled during the testing phase; aliquots were thawed only once and transduction and infectivity assays were performed within 1 hr of this thaw. Regarding future use of the reference material for potency assays, it would seem essential that a similar protocol be followed when normalizing internal reference standards against the rAAV2 RSM. For physical titer assays such as particle and vector genome assays, storage and refreezing are permissible. Plans for assessing the long-term stability of the rAAV2 RSM by yearly testing for capsid protein integrity, infectious titer, transducing titer, and vector genome titer are in place. Data will be reported by the AAV2RSWG through the Reference Standards section of the International Society for BioProcess Technology website (www.ISBioTech.org).

The characterization phase of the rAAV2 RSM project successfully fulfilled the goals of the AAV2RSWG by obtaining mean titers and 95% confidence intervals from a large number of representative assays performed by numerous test centers. The tightest confidence intervals were obtained for the nonbiological assays (particle titer and vector genome titer) whereas the biological assays (infectious titer and transduction titer) gave wider intervals (Table 5). This pattern might be expected because the biological assays are inherently more variable. The tight confidence interval observed for the vector genome titer is relevant because this titer has been used exclusively in dosing regimens and a high degree of precision is important for the use of the rAAV2 RSM in dose standardization.

One obvious trend in the quantitative assay data was the degree of variation between institutions for each assay (Fig. 1 and Table 3) despite the relatively tight correlation of assay results within an institution (Table 3). This poor degree of interlaboratory precision and accuracy was apparent even though attempts were made to standardize the assays by providing detailed protocols and common reagents. The variation may be explained by the use of different reagents (i.e., other than those provided, such as tissue culture media, PCR primers, and PCR mixes), equipment, and/or operator technique. This is the first time that such variation between laboratories has been thoroughly documented and the find-

ings emphasize the need in the field for universal reference standards. This need is especially apparent when it is considered that fundamentally dissimilar tests are often used to measure the same parameter (e.g., qPCR and dot-blot for vector genome titer) and that even when different laboratories use the same assay, different protocols are usually followed. For some assays the variation is not large, with the most important measure, vector genome titer (qPCR), which is almost exclusively used for dosing in preclinical and clinical studies, having low variation (confidence interval of less than 0.5 log). Despite the spread of infectious titers, the mean value represents the best titer based on multiple replicates conducted at the different sites on different test dates.

Because the rAAV2 RSM supply is limited, it is not intended that it be used routinely, but rather for the calibration of laboratory-specific internal reference standards, which can then be run concurrently with test samples in subsequent assays that have been validated. The initial calibration would involve titrating the RSM alongside the internal standard in the same assay; the difference between the titer determined in this assay and the accepted titer of the RSM would act as a conversion factor for calculating the titer of the internal standard in reference standard units (RSU). Once the internal standard titer is known in reference standard units per milliliter, the titer of test samples can be calculated similarly in the same units, during subsequent assays. It is envisaged that the RSM will be used in this way for standardizing the genome titer, particle titer, and infectious titer of AAV2 vectors. A prerequisite for qPCR or hybridization-based vector genome/infectivity titrating methods would be that the internal AAV standard share enough genome sequence with the rAAV2 RSM for oligonucleotide or labeled probe annealing. Several common transcriptional elements are included in the rAAV2 RSM genome for this purpose and many existing internal reference standards will therefore be candidates for calibration. If this is not the case, new internal standards will need to be produced that harbor DNA elements in common with the AAV2 RSM. For transducing titers, the encoded transgene provides the basis of detection and, therefore, with the exception of GFP-expressing vectors for preclinical studies, these titers will generally not be amenable to standardization using the rAAV2 RSM.

Although the primary intent of the rAAV2 RSM was to provide a reference point for AAV2 serotype vectors it is possible that for nonbiological assays such as vector genome titration, the rAAV2 RSM could be used for the calibration of other AAV serotypes. Because the vector capsid is not directly involved in these types of assays, it might be argued that there is no capsid specificity and that the capsid serotype would not have an impact. As an example, in the vector genome titer assay it might be assumed that different capsids are equally susceptible to PCR heat treatment for liberation of the vector genome. However, conditions would need to be optimized because equal susceptibility of AAV serotypes to heat has not been definitively demonstrated. In addition, proteolysis is often used to liberate the vector genome and it is known that different capsid serotypes have different susceptibilities to protease treatments (Van Vliet *et al.*, 2006). Similarly, serotype-independent methods of determining particle titer (e.g., high-performance liquid chromatography, spectrophotometry) could be calibrated, using the rAAV2 RSM, but the same assumption of capsid independence

would apply, and for spectrophotometric measurements the proper extinction coefficient would need to be incorporated (Sommer *et al.*, 2003). If data are available to demonstrate that an assay is indeed capsid independent, then the use of the rAAV2 RSM for other serotypes may well be acceptable, but thorough review with the appropriate regulatory agency is recommended. For biological assays such as infectious titer, the paramount roles of the capsid, the requisite target cell line, and the helper virus preclude the use of the rAAV2 RSM to calibrate other serotypes. For these assays, investigators must await the development of further reference standard materials such as the AAV8 material currently under production (Moullier and Snyder, 2008).

The rAAV2 RSM carries a single-stranded DNA vector genome. Self-complementary AAV vector genomes, generated with a mutation within the terminal repeat (McCarty *et al.*, 2003), have become popular for gene transfer because they bypass the rate-limiting genome conversion of single-stranded to double-stranded DNA during transduction of target cells. The rAAV2 RSM can be used to normalize "in-house" reference standards for both the classic single-stranded vectors and self-complementary vectors. Because self-complementary vectors carry double the genome complement of single-stranded vectors, a simple conversion is necessary when calculating vector genome titers for these two vector types.

In the United States, the FDA Center for Biologics Evaluation and Research (CBER), Office of Cellular, Tissue, and Gene Therapies (OCTGT), Division of Cellular and Gene Therapies (DCGT) recommends reference materials as benchmarking tools for qualifying and validating "in-house" reference standards and assays by comparison with the collective data. It should be noted that it is not the intent of the FDA to standardize assay methods across the field or to require that the values assigned to the rAAV2RSM be duplicated during validation studies. Furthermore, there is no requirement in the United States to follow rAAV2 RSM procedures when assaying particle concentration, genome copy number, or infectious titer. Sponsors of adeno-associated virus-related investigational new drugs (INDs) should consult with the FDA/CBER or appropriate national agency for further guidance. The rAAV2 RSM fulfills many of the requirements of a reference standard material in that it (1) is sufficiently homogeneous and stable with respect to specified properties, (2) is established to be fit for its intended use in measurement, (3) is accompanied by documentation, (4) provides relevant property values that are based on multiple measurements conducted at different locations, and (5) is accompanied with associated measurement uncertainty.

From the outset, the vision of the AAV2RSWG for the rAAV2 RSM was that it would represent the first step toward standardization of AAV-based gene therapy dosing and provide a blueprint for the development of reference standards for other AAV serotypes. This vision is becoming reality through the successful production and characterization reported here, and with the effort to develop the AAV8 reference standard material underway. The requirement that the reference materials be universally accepted by the AAV community has dictated the need for a voluntary communal effort in the production and characterization phases. Despite the numerous drawbacks, difficulties, and delays inherent in this type of approach, the AAV gene therapy community has

responded selflessly and with enthusiasm. It is hoped that the ultimate success of this collaboration will inspire future reference standard efforts and contribute to the development and commercialization of AAV-based gene therapeutics.

Acknowledgments

Current and former members of the Executive Committee: Denise Gavin–FDA (nonvoting member); Daniel Rosenblum–NIH NCRR (nonvoting member); Keith Carson–International Society for BioProcess Technology; Parris Burd–Bayer Corporation; Olivier Danos–Généthon; Maritza McIntyre–FDA (nonvoting member); Richard Knazek–NIH NCRR (nonvoting member). Manufacturing committee: Guang Ping Gao–University of Pennsylvania; Philip Cross–Harvard Medical School; Anna Salvetti–CHU Hôtel Dieu, Nantes, France; Sue Washer–Applied Genetic Technologies; Guang Qu–Avigen. Quality committee: Marie Printz–Ceregene; Paul Husak–Cell Genesys; Scott McPhee–Thomas Jefferson University; Jurg Sommer–Avigen; Jim Marich–Cell Genesys. We acknowledge the technical help of the following during the testing phase: Mark Potter–PGTC Vector Core; Gitte Kitlen–PGTC Quality Control; Lynn Combee–PGTC Toxicology Core; Cheryl Roberts–PGTC Toxicology Core; Tanja Finnäs–AMT; Martha Hoekstra–AMT. We are grateful to James Wilson–University of Pennsylvania for supporting the beta testing through NIH grant P30-DK-047757 and an SRA from GlaxoSmithKline. We are also indebted to Peggy Fahnstock and Liz Kerrigan at the ATCC for coordinating the distribution of materials to testing laboratories. This work was supported by NIH grant U42RR11148. We acknowledge the generosity of the ATCC, Nunc, Aldevron, Corning, Fisher Thermo Scientific, the Indiana University Vector Production Facility, HyClone, Mediatech, Progen, and the Williamsburg Bioprocessing Foundation. Richard Surosky is employed by a company that may have interest in these vectors for therapeutic purposes. Richard Snyder owns equity in a gene therapy company that is commercializing AAV for gene therapy applications.

References

- Brantly, M.L., Chulay, J.D., Wang, L., Mueller, C., Humphries, M., Spencer, L.T., Rouhani, F., Corlon, T.J., Calcedo, R., Betts, M.R., Spencer, C., Byrne, B.J., Wilson, J.M., and Flotte, T.R. (2009). Sustained transgene expression despite T lymphocyte responses in a clinical trial of rAAV1-AAAT gene therapy. *Proc. Natl. Acad. Sci. U.S.A.* 106, 16363–16368.
- Burger, C., Gorbatyuk, O.S., Velardo, M.J., Peden, C.S., Williams, P., Zolotukhin, S., Reier, P.J., Mandel, R.J., and Muzyczka, N. (2004). Recombinant AAV viral vectors pseudotyped with viral capsids from serotypes 1, 2, and 5 display differential efficiency and cell tropism after delivery to different regions of the central nervous system. *Mol. Ther.* 10, 302–317.
- CBER/FDA (Center for Biologics Evaluation and Research, U.S. Food and Drug Administration). (1993). Points to consider in the characterization of cell lines used to produce biologicals. Available at <http://www.fda.gov/downloads/BiologicsBloodVaccines/GuidanceComplianceRegulatoryInformation/OtherRecommendationsforManufacturers/UCM062745.pdf> (accessed July 2010).
- Chadeuf, G., Favre, D., Tessier, J., Provost, N., Nony, P., Kleinschmidt, J., Moullier, P., and Salvetti, A. (2000). Efficient

- recombinant adeno-associated virus production by a stable rep-cap HeLa cell line correlates with adenovirus-induced amplification of the integrated rep-cap genome. *J. Gene Med.* 2, 260–268.
- Croyle, M.A., Cheng, X., and Wilson, J.M. (2001). Development of formulations that enhance physical stability of viral vectors for gene therapy. *Gene Ther.* 8, 1281–1290.
- Grimm, D., Kern, A., Rittner, K., and Kleinschmidt, J.A. (1998). Novel tools for production and purification of recombinant adenoassociated virus vectors. *Hum. Gene Ther.* 9, 2745–2760.
- Hutchins, B. (2002). Development of a reference material for characterizing adenovirus vectors. *BioProcess. J.* 1, 25–28.
- Kärber, G. (1931). 50% end-point calculation. *Arch. Exp. Pathol. Pharmacol.* 162, 480–483.
- Littell, R.C., Milliken, G.A., Stroup, W.W., and Wolfinger, R.E. (2006). *SAS for Mixed Models*, 2nd ed. (SAS Institute, Cary, NC).
- Maguire, A.M., Simonelli, F., Pierce, E.A., Pugh, E.N., Jr., Mingozzi, F., Bannicelli, J., Banfi, S., Marshall, K.A., Testa, F., Surace, E.M., Rossi, S., Lyubarsky, A., Arruda, V.R., Konkle, B., Stone, E., Sun, J., Jacobs, J., Dell'Osso, L., Hertle, R., Ma, J.X., Redmond, T.M., Zhu, X., Hauck, B., Zelenaiia, O., Shindler, K.S., Maguire, M.G., Wright, J.F., Volpe, N.J., McDonnell, J.W., Auricchio, A., High, K.A., and Bennett, J. (2008). Safety and efficacy of gene transfer for Leber's congenital amaurosis. *N. Engl. J. Med.* 358, 2240–2248.
- McCarty, D.M., Fu, H., Monahan, P.E., Toulson, C.E., Naik, P., and Samulski, R.J. (2003). Adeno-associated virus terminal repeat (TR) mutant generates self-complementary vectors to overcome the rate-limiting step to transduction *in vivo*. *Gene Ther.* 10, 2112–2118.
- Moss, R.B., Rodman, D., Spencer, L.T., Aitken, M.L., Zeitlin, P.L., Waltz, D., Milla, C., Brody, A.S., Clancy, J.P., Ramsey, B., Hamblett, N., and Heald, A.E. (2004). Repeated adeno-associated virus serotype 2 aerosol-mediated cystic fibrosis transmembrane regulator gene transfer to the lungs of patients with cystic fibrosis: A multicenter, double-blind, placebo-controlled trial. *Chest* 125, 509–521.
- Moullier, P., and Snyder, R.O. (2008). International efforts for recombinant adeno-associated viral vector reference standards. *Mol. Ther.* 16, 1185–1188.
- Mueller, C., and Flotte, T.R. (2008). Clinical gene therapy using recombinant adeno-associated virus vectors. *Gene Ther.* 15, 858–863.
- Nienhuis, A. (2009). Dose-escalation study of a self complementary adeno-associated viral vector for gene transfer in hemophilia B. Clinical trial NCT00979238. Available at <http://clinicaltrials.gov/ct2/show/NCT00979238> (accessed July 2010).
- Potter, M., Phillipsberg, G., Phillipsberg, T., Pettersen, M., Sanders, D., Korytov, I., Fife, J., Zolotukhin, S., Byrne, B.J., and Muzyczka, N. (2008). Manufacture and stability study of the recombinant adeno-associated virus serotype 2 vector reference standard. *BioProcess. J.* 7, 8–14.
- Rabilloud, T., Strub, J.M., Luche, S., van Dorsselaer, A., and Lunardi, J. (2001). A comparison between SYPRO Ruby and ruthenium II tris(bathophenanthroline disulfonate) as fluorescent stains for protein detection in gels. *Proteomics* 1, 699–704.
- Salveti, A., Oreve, S., Chadeuf, G., Favre, D., Cherel, Y., Champion-Arnaud, P., David-Ameline, J., and Moullier, P. (1998). Factors influencing recombinant adeno-associated virus production. *Hum. Gene Ther.* 9, 695–706.
- Snyder, R.O., and Flotte, T.R. (2002). Production of clinical-grade recombinant adeno-associated virus vectors. *Curr. Opin. Biotechnol.* 13, 418–423.
- Sommer, J.M., Smith, P.H., Parthasarathy, S., Isaacs, J., Vijay, S., Kieran, J., Powell, S.K., McClelland, A., and Wright, J.F. (2003). Quantification of adeno-associated virus particles and empty capsids by optical density measurement. *Mol. Ther.* 7, 122–128.
- Van Vliet, K., Blouin, V., Agbandje-McKenna, M., and Snyder, R.O. (2006). Proteolytic mapping of the adeno-associated virus capsid. *Mol. Ther.* 14, 809–821.
- Warrington, K.H., Jr., and Herzog, R.W. (2006). Treatment of human disease by adeno-associated viral gene transfer. *Hum. Genet.* 119, 571–603.
- Weiss, W., Weiland, F., and Gorg, A. (2009). Protein detection and quantitation technologies for gel-based proteome analysis. *Methods Mol. Biol.* 564, 59–82.
- Wright, J.F., Qu, G., Tang, C., and Sommer, J.M. (2003). Recombinant adeno-associated virus: Formulation challenges and strategies for a gene therapy vector. *Curr. Opin. Drug Discov. Dev.* 6, 174–178.
- Zen, Z., Espinoza, Y., Bleu, T., Sommer, J.M., and Wright, J.F. (2004). Infectious titer assay for adeno-associated virus vectors with sensitivity sufficient to detect single infectious events. *Hum. Gene Ther.* 15, 709–715.
- Zolotukhin, S., Byrne, B.J., Mason, E., Zolotukhin, I., Potter, M., Chesnut, K., Summerford, C., Samulski, R.J., and Muzyczka, N. (1999). Recombinant adeno-associated virus purification using novel methods improves infectious titer and yield. *Gene Ther.* 6, 973–985.

Address correspondence to:

Dr. Richard O. Snyder

Department of Molecular Genetics and Microbiology

1600 SW Archer Road

Gainesville, FL 32610-0266

E-mail: rsnyder@cerhb.ufl.edu

Received for publication December 21, 2009;

accepted after revision May 18, 2010.

Published online: August 25, 2010.

This article has been cited by:

1. W Ni, C Le Guiner, G Gernoux, M Penaud-Budloo, P Moullier, R O Snyder. 2011. Longevity of rAAV vector and plasmid DNA in blood after intramuscular injection in nonhuman primates: implications for gene doping. *Gene Therapy* . [CrossRef]
2. V. Jimenez, E. Ayuso, C. Mallol, J. Agudo, A. Casellas, M. Obach, S. Muñoz, A. Salavert, F. Bosch. 2011. In vivo genetic engineering of murine pancreatic beta cells mediated by single-stranded adeno-associated viral vectors of serotypes 6, 8 and 9. *Diabetologia* . [CrossRef]
3. Cormac Sheridan. 2011. Gene therapy finds its niche. *Nature Biotechnology* 29:2, 121-128. [CrossRef]

Characterisation of an antibody specific for coagulation factor VIII that enhances factor VIII activity

Masahiro Takeyama¹; Keiji Nogami¹; Tomoko Matsumoto¹; Tetsuhiro Soeda²; Tsukasa Suzuki²; Kunihiro Hattori²; Midori Shima¹

¹Department of Pediatrics, Nara Medical University, Kashihara, Nara, Japan; ²Chugai Pharmaceutical Co. Ltd., Fuji-Gotemba Research Laboratories, Gotemba, Shizuoka, Japan

Summary

Many reports have identified factor (F)VIII inhibitory antibodies with epitopes located in all subunits of the FVIII molecule. Antibodies that promote FVIII activity do not appear to have been reported. We characterised, for the first time, a unique anti-FVIII monoclonal antibody, mAb216, that enhanced FVIII coagulant activity. The mAb216 shortened the activated partial thromboplastin time and specifically increased FVIII activity by ~1.5-fold dose-dependently. FXa generation and thrombin generation were similarly increased by ~1.4- and ~2.5-fold, respectively. An A2 epitope, not overlapping the common A2 epitope, was identified and the antibody was shown to enhance thrombin (and FXa)-catalysed activation of FVIII by modestly accelerating cleavage at Arg³⁷². The presence of mAb216 mediated an ~1.5-fold de-

crease in K_m for the FVIII-thrombin interaction. Enhanced FVIII activity was evident to an equal degree, even the presence of anti-FVIII neutralising antibodies with epitopes in each subunit. In addition, mAb216 depressed the rates of heat-denatured loss of FVIII activity and FVIIIa decay by 2 to ~2.5-fold. We have developed an anti-A2, FVIII mAb216 that augmented procoagulant activity. This enhancing effect could be attributed to an increase in thrombin-induced activation of FVIII, mediated by cleavage at Arg³⁷² and a tighter interaction of thrombin with the A2 domain. The findings may cast new light on new principles for improving the treatment of haemophilia A patients.

Keywords

A2 epitope, enhancing antibody, FVIII activation, stability, thrombin

Correspondence to:

Keiji Nogami, MD, PhD
Department of Pediatrics, Nara Medical University
840 Shijo-cho, Kashihara, Nara 634-8522, Japan
Tel.: +81 744 29 8881, Fax: +81 744 24 9222
E-mail: roc-noga@naramed-u.ac.jp

Financial support:

This work was supported in part by MEXT KAKENHI Grant (19591264 and 21591370) and The Mother and Child Health Foundation.

Received: May 30, 2009

Accepted after major revision: August 11, 2009

Prepublished online: September 30, 2009

doi:10.1160/TH09-05-0338

Thromb Haemost 2010; 103: 94–102

Introduction

Factor (F)VIII circulates as a complex with von Willebrand factor (VWF) and functions as an essential cofactor in the FXase complex responsible for phospholipid surface-dependent conversion of FX to FXa by FIXa (1). Molecular defects in FVIII result in the congenital bleeding disorder, haemophilia A. FVIII is composed of 2,332 amino acid residues (~300 kDa), and contains three types of domain, arranged in the order of A1-A2-B-A3-C1-C2 (2). Mature FVIII is processed to a series of metal ion-dependent heterodimers by cleavage at the B-A3 junction, generating a heavy chain (HCh) consisting of the A1 and A2 domains, together with heterogeneous fragments of the B domain, linked to a light chain (LCh) consisting of the A3, C1, and C2 domains. FVIII is converted into an active form, FVIIIa, by limited proteolysis catalysed by either thrombin or FXa (3). Cleavages at Arg³⁷² and Arg⁷⁴⁰ in HCh produce 50-kDa A1 and 40-kDa A2 subunits. Cleavage of the 80-kDa LCh at Arg¹⁶⁸⁹ produces a 70-kDa A3-C1-C2 subunit. Mutational analyses listed in the International Hemophilia A database indicate that proteoly-

sis at Arg³⁷² and Arg¹⁶⁸⁹ is essential for generating FVIIIa cofactor activity (4).

FVIII inhibitors develop as alloantibodies (alloAbs) in ~20% of multi-transfused patients with haemophilia A. Epitopes of these neutralising antibodies have been located within each of the FVIII domains, but predominantly in the A2, C2, and A3-C1 domains (5). Most antibodies recognising the C2 domain prevent FVIII binding to VWF (6) and phospholipid (7), and some inhibit FVIII activation by thrombin (8) and FXa (9). Most antibodies recognising the A2 or A3-C1 domain inhibit FVIIIa-FIXa interaction in the FXase complex (10, 11). These findings indicate that inactivation of FVIII activity by the inhibitory antibodies is related to impairment of cofactor function by the occupation of functionally important regions in the FVIII molecule. Epitope localisation and characterisation of these antibodies can provide useful information on FVIII(a) structure and function.

In contrast, in this study, we have identified a non-inhibitory anti-FVIII monoclonal antibody (mAb), mAb216, that bound to FVIII and enhanced its activity. The antibody recognised the A2

domain but not the common A2 inhibitor epitopes. The enhanced mechanism was attributed to an acceleration of the cleavage of Arg³⁷² in the FVIII HCh, mediated by the binding of mAb216 to the A2 domain. Enhanced activity was observed even the presence of anti-FVIII inhibitory antibodies. The findings may offer a challenging new principle for improving the treatment of haemophilia A patients with and without inhibitors.

Materials and methods

Reagents

Recombinant FVIII (Kogenate FS[®]) was a generous gift from Bayer Corp. Japan (Osaka, Japan). The LCh and HCh, A1, and A2 subunits were isolated as previously reported (12). SDS-PAGE of the isolated subunits followed by staining with GelCode BlueStain Reagent (Pierce, Rockford, IL, USA) showed >95% purity. Coagtrol N, FVIII-deficient plasmas (Sysmex, Kobe, Japan), human α -thrombin, FIXa, FX, FXa (Hematologic Technologies, Burlington, VT, USA), and recombinant human tissue factor (rTF; Innovin[®], Dade Behring, Newark, DE, USA), fluorogenic specific-substrate for thrombin, Z-Gly-Gly-Arg-AMC (Bachem, Bubendorf, Switzerland), and chromogenic FXa substrate S-2222 (Chromogenix, Milano, Italy) were purchased from the indicated manufacturers. Phospholipid vesicles containing 10% phosphatidylserine, 60% phosphatidylcholine, and 30% phosphatidylethanolamine (Sigma) were prepared using *N*-octylglucoside (13).

Antibodies

A series of anti-FVIII mAbs were generated by standard hybridoma procedures. Briefly, spleen cells were isolated from mice immunised with human FVIII and fused with murine myeloma P3U1 cells. The fused cells were cultured in HAT selection medium (hypoxanthine/aminopterin/thymidine). Aliquots of culture supernatants were screened for FVIII binding by enzyme-linked immunosorbent assay (ELISA). Relevant antibody-secreting hybridoma cells were selected and cloned by limited dilution twice to maximise monoclonality. The cloned mAbs were purified using Protein G Sepharose (Amersham Bio-Science). The effects of the mAbs on blood coagulation were examined in activated partial thromboplastin time (APTT)-assays. The mAbC5 with an A1 epitope (12) and the mAb413 with an A2 epitope (10) were kindly provided by Dr. C. A. Fulcher and Dr. E. L. Saenko, respectively. The anti-C2 mAbNMC-VIII/5 was purified as previously reported (14). Anti-A3 mAbJR5 and anti-A2 JR8 were obtained from JR Scientific Inc. (Woodland, CA, USA). FVIII epitopes were determined by ELISA and surface plasmon resonance (SPR)-based assay (Biacore X[™]) (8, 9). Biotinylated IgG was prepared using *N*-hydroxysuccinimido-biotin (Pierce). F(ab')₂ was prepared using ImmunoPure F(ab')₂ preparation Kit (Pierce).

Clotting assays

Normal plasma was mixed with mAb216 and evaluated by APTT clot waveform analysis (15). Transmittances were monitored during the APTT measurement, and clot waveform parameters (clotting time, maximum coagulation velocity [min I]) were calculated by the MDA-II[™] system (Trinity Biotech, CW, Ireland). Specific FVIII activity was measured in a one-stage clotting assay using FVIII-deficient plasma. For assessing FVIII heat-stability, purified FVIII (1 nM) or normal plasma was incubated at 55 °C. FVIII activity was measured at intervals in a one-stage clotting assay.

FXa generation assay

The rate of conversion of FX to FXa was monitored in purified systems (16). FVIII (30 nM) was activated by thrombin at the indicated concentrations in the presence of phospholipid (10 μ M). The thrombin reaction was terminated after 1 minute (min) by the addition of hirudin. FXa generation was initiated by the addition of FIXa (0.5 nM) and FX (300 nM). Aliquots were removed at appropriate times to assess initial rates of product formation and added to tubes containing EDTA to stop the reaction. Rates of FXa generation were determined by adding of chromogenic substrate S-2222 (0.46 mM final concentration). Reactions were read at 405 nm using a Multiskan microplate reader (Labsystems, Helsinki, Finland).

Thrombin generation assay

The amount of thrombin generated in plasma was measured by calibrated automated thrombography (17). Normal plasma was preincubated with various concentrations of mAb216 for 2 hours (h) at 37°C. Plasma mixtures were incubated in microtiter wells with mixtures of rTF and phospholipid vesicles in 20 mM HEPES, 0.1 M NaCl, 5 mM CaCl₂, and 0.01% Tween 20, pH 7.2 (HBS-buffer). The reaction was initiated by the addition of CaCl₂ and rates of thrombin generation were determined using fluorogenic thrombin substrate. All reagents were prewarmed to 37°C. Final concentrations of reagents were 0.5 pM rTF, 4 μ M phospholipid, 433 μ M fluorogenic substrate, and 13.3 mM CaCl₂. The fluorescent signal was monitored at 8-second (s) intervals using a Fluoroskan Ascent microplate reader (Thermo Electron Co., Waltham, MA, USA) with a 390 nm (excitation)/460 nm (emission) filter set. Fluorescent signals were corrected and actual thrombin generation (in nM) was calculated by reference to thrombin calibrator samples.

FVIII activation and cleavage

Activation and cleavage of FVIII by thrombin and FXa was assessed as previously reported (8, 9). FVIII (100 nM) was incubated with

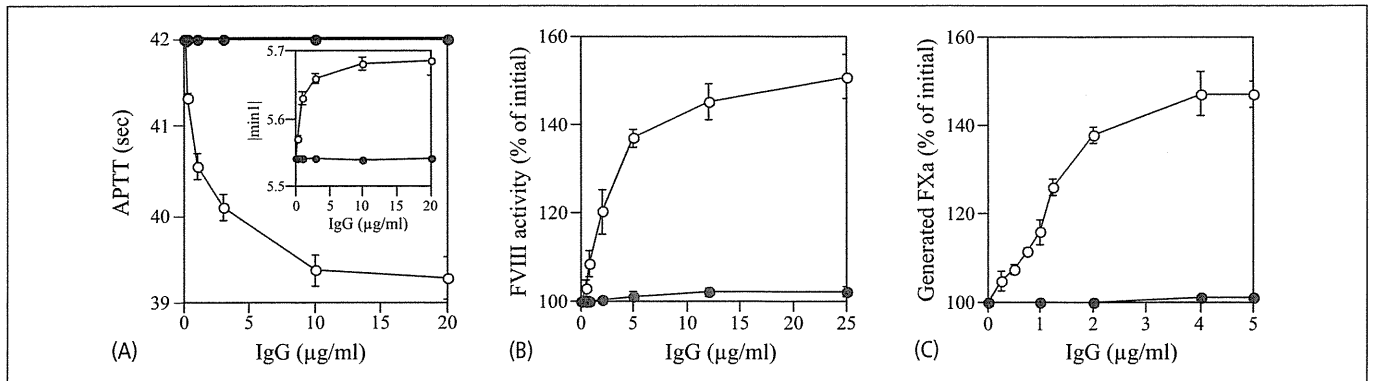


Figure 1: Effects of mAb216 on the APTT and FVIII coagulant activity. A) Clot time. Normal plasma was incubated with mAb216 (○) or normal IgG (●) prior to measuring the APTT in clot waveform assays. Inset shows the |min1| calculated from clot waveform patterns. B) FVIII activity: FVIII (1 nM) was incubated with mAb216 (○) or normal IgG (●) and FVIII activity was measured in one-stage clotting assays. FVIII activity in the absence of

mAb216 represents the initial level (100%). C) FVIIIa-dependent FXa generation. FVIII (30 nM) was incubated with mAb216 (○) or normal IgG (●) prior to activation with thrombin (10 nM). FXa generation was initiated by adding FIXa (0.5 nM) and FX (300 nM). FXa generated in the absence of mAb216 represents the 100% level (~160 nM/min). Experiments were performed five separate times, and the average values and standard deviations are shown.

thrombin or FXa plus 10 µM phospholipid in HBS-buffer at 37°C. Samples were removed at the indicated intervals and reactions immediately terminated by 5,000-fold dilution on ice, adding SDS-buffer and boiling. The presence of thrombin and FXa in diluted samples did not affect these assays.

The half-life values were calculated from Equation 2.

$$t_{1/2} = 10^C \times \ln(2)$$

where C is $-\log k$, as in Equation 2.

Electrophoresis and Western blotting

SDS-PAGE, using 8% gels, and Western blot analyses were performed as previously reported (12). Densitometry scans were quantified using Image J 1.34 software (National Institutes of Health, Bethesda, MD, USA).

Data analyses

All experiments were performed at least three separate times, and the average values and standard deviations (SD) were calculated. Non-linear least squares regression analysis was performed using KaleidaGraph (Synergy Software, Reading, PA, USA). The K_m and k_{cat} values for FVIIIa/FIXa-catalysed FX activation were calculated from the Michaelis-Menten equation.

Analysis of the intramolecular stability of FVIII was determined by Equation 1.

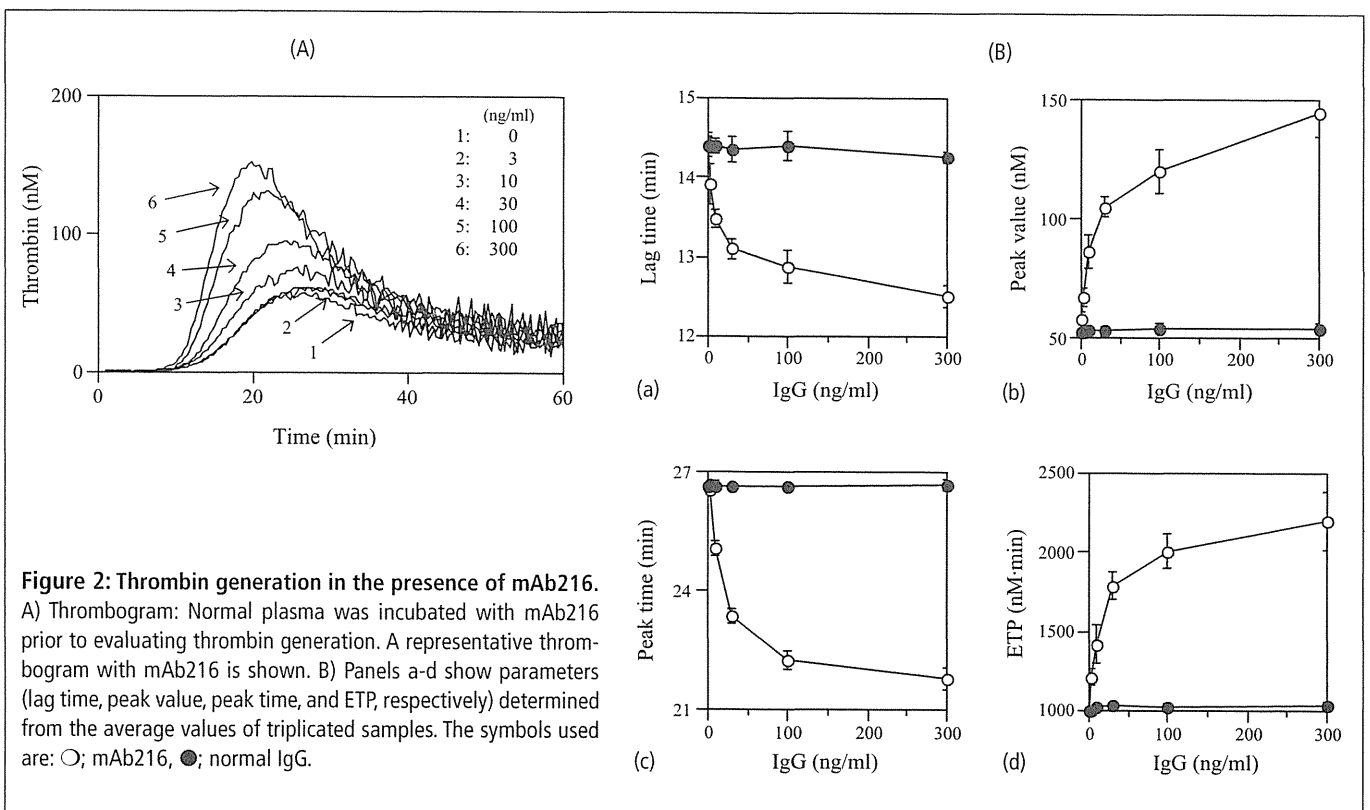
$$[FVIII]_t = [FVIII]_0 \cdot e^{(-10^C \times t)}$$

where $[FVIII]_0$ and $[FVIII]_t$ represents concentrations at initial (0) and time point (t), respectively, and C is $-\log k$, with rate constant k.

Results

Effect of mAb216 on APTT and FVIII activity

The effects of the various anti-FVIII mAb preparations on the APTT were evaluated using clot waveform analysis (15). Only one antibody (numbered mAb216) when preincubated with normal plasma shortened the APTT. The effect was modest but dose-dependent, with a ~3 s difference at 10 µg/ml (► Fig. 1A). The |min1| value of the clot waveform analysis was correspondingly increased (inset). To further examine this acceleration of procoagulant activity, we assessed the effect of mAb216 specifically on FVIII activity. Purified FVIII (1 nM) was preincubated with mAb216 and FVIII activity measured at intervals in a one-stage clotting assay. FVIII activity in the presence of mAb216 was increased by ~1.5-fold at 12.5 µg/ml compared to control IgG, and this effect was dose-dependent (Fig. 1B). In addition, FXa generation assays using purified components showed that mAb216 increased FVIIIa/FIXa-dependent FXa generation by ~1.5-fold dose-dependently (Fig. 1C). Similar results were obtained using F(ab')₂ preparations (data not shown). The results indicated that the enhanced procoagulant activity mediated by mAb216 was related to an increase in FVIII activity.



Thrombin generation in the presence of mAb216

Measurements of thrombin generation in plasma are reported to correlate with coagulant ability and to be clinically useful (17). Furthermore, levels of FVIII activity appear to correlate with that of thrombin generation (18). We evaluated, therefore, the effects of mAb216 on thrombin generation using plasma. Thrombin generation assay in the presence of TF (5 pM) showed that the enhancing effect of mAb216 was mildly less than expected (data not shown). Therefore, to observe the significant difference, assays were performed at low concentrations of rTF (0.5 pM) and phospholipid (4 μ M) as previously recommended (19). As shown in Figure 2A, thrombin generation was increased in the presence of mAb216 dose-dependently. Four parameters of thrombin generation (lag time, peak value, peak time, and endogenous thrombin potential [ETP]) were calculated (Fig. 2B a-d, respectively). The addition of mAb216 shortened the lag time and peak time, and increased the peak value and ETP by 2- to ~3-fold at 0.3 μ g/ml concentration. Control experiments using FVIII-deficient plasma demonstrated that mAb216 itself did not affect thrombin generation, indicating that the enhancing effect of mAb216 attributed to the presence of FVIII (data not shown). The data were consistent with the results showing that mAb216 increased FVIII activity. However, low concentration of TF may be not the driver of thrombin generation, rather contact activation under such circumstances. To avoid this influence, thrombin generation assay trig-

gered by TF (0.5 pM) was performed in the presence of corn trypsin inhibitor. Results obtained in the presence of corn trypsin inhibitor were almost similar to that in its absence (data not shown), supportive of validity of this assay using lower TF. Furthermore, an effective concentration of mAb216 obtained in this assay was lower, compared to that in APTT (Fig. 1A, B) or FXa generation assay (Fig. 1C). This reason is unclear, but may be due to difference of assay.

In order to identify the epitope recognised by mAb216, we performed ELISA in which different FVIII(a) subunits were immobilized onto microtiter wells. The mAb216 bound to immobilized FVIII, HCh, and A2 domain, and not to LCh and A1 domain. In addition, SPR-based assays also demonstrated that FVIII bound to mAb216 immobilised on a sensor chip (K_D : 1.1 nM, k_{ass}/k_{diss} : $9.3 \times 10^5 \text{ M}^{-1}\text{s}^{-1}/1.0 \times 10^{-3} \text{ s}^{-1}$), and in keeping with the ELISA results, the HCh and A2 domain bound to solid phase antibody (K_D : 3.0 and 0.8 nM, k_{ass}/k_{diss} : $2.9 \times 10^5 \text{ M}^{-1}\text{s}^{-1}/0.9 \times 10^{-3} \text{ s}^{-1}$ and $2.4 \times 10^5 \text{ M}^{-1}\text{s}^{-1}/0.2 \times 10^{-3} \text{ s}^{-1}$), whilst LCh and A1 failed to bind. The results confirmed that mAb216 possessed an A2 epitope. Furthermore, competition experiments using the ELISA method demonstrated that the A2 epitope of mAb216 did not overlap with the common epitope (residues 484–509) represented by anti-A2 mAb413 (data not shown).

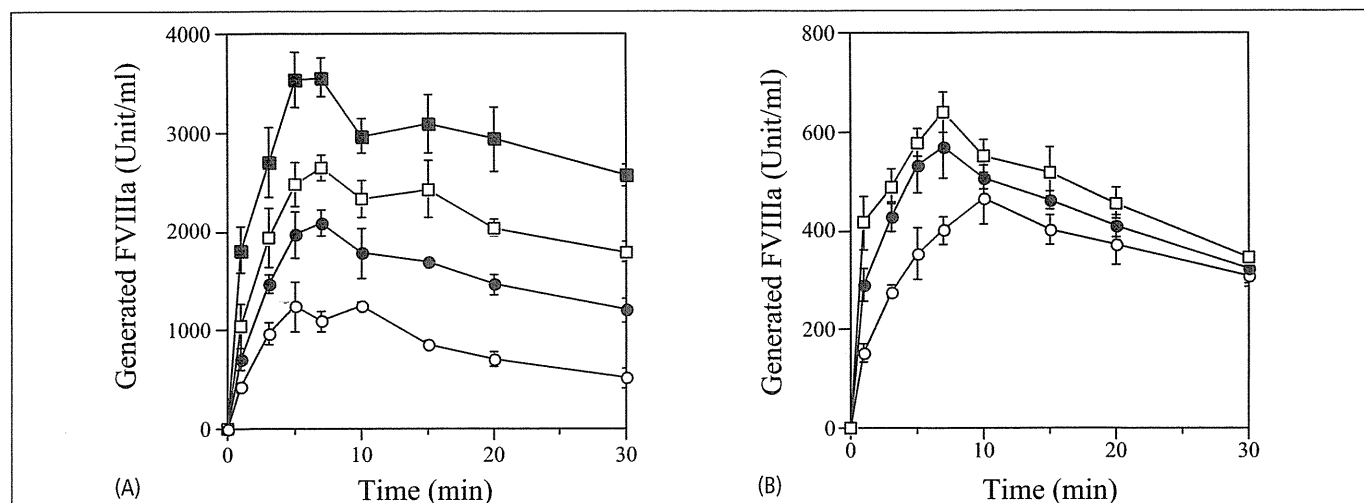


Figure 3: Effect of mAb216 on thrombin- or FXa-catalysed FVIII activation. FVIII (100 nM) was preincubated with mAb216 and was activated by thrombin (1 nM, A) or FXa (4 nM, B) plus phospholipid (10 μM). FVIII activity was measured at the indicated time intervals in one-stage clotting assays. The symbol used are (A) ○; 0 μg/ml, ●; 2.5 μg/ml, □; 5 μg/ml, ■; 10 μg/ml, (B) ○; 0 μg/ml, ●; 10 μg/ml, □; 20 μg/ml. Experiments were performed three separate times, and the average values and standard deviations are shown.

mAb216 affects FVIII activation and proteolytic cleavage by thrombin and FXa

To clarify the mechanism(s) by which mAb216 enhances FVIII activity, we focused on FVIII activation by thrombin and/or FXa. FVIII was incubated with mAb216 prior to incubation with thrombin or FXa, and FVIIIa activity was assayed at timed intervals. Peak levels of FVIIIa activity induced by thrombin were significantly increased, dose-dependently, in the presence of mAb216 (► Fig. 3A). The presence of mAb216 (10 μg/ml) showed an ~3-fold elevation of peak level of FVIIIa activity. Similarly, peak levels of FXa-induced FVIII activation with mAb216 were increased dose-dependently (Fig. 3B). The presence of mAb216 (10 μg/ml) showed an ~1.4-fold elevation of FVIIIa activity, although the effect of FXa on FVIII activation was not dominant in these circumstances, compared to that of thrombin. Overall these results clearly indicated that mAb216 enhanced FVIII activation by thrombin (and FXa)- related mechanisms.

The generation of FVIIIa activity is regulated by proteolytic cleavage at Arg³⁷² at the A1-A2 junction (3). Since both thrombin and FXa cleave FVIII at Arg³⁷², we speculated that the FVIII-enhancing effect of mAb216 might be due to the acceleration of Arg³⁷² cleavage. In order to confirm this, we examined the effect of mAb216 on thrombin- (and FXa-) catalysed HCh cleavage by SDS-PAGE. Western blotting (► Fig. 4A panels a,b) and band densitometry (panel c) demonstrated that mAb216 mildly accelerated cleavage by thrombin at the A1-A2 junction (Arg³⁷²) but did not appreciably affect cleavage at the A2-B junction (Arg⁷⁴⁰). The ratio of the A2/A1-A2 product obtained by densitometry suggested that cleavage at Arg³⁷² in the presence of mAb216 was faster than that of control by ~2-fold. This finding was similar to that observed with thrombin-catalysed activation. However, LCh cleavage by thrombin at Arg¹⁶⁸⁹ was not significantly affected (data not shown).

Similarly, cleavage at Arg³⁷² by FXa was mildly accelerated by mAb216, whilst that at Arg⁷⁴⁰ was little affected (Fig. 4B). The cleavage rate (A2/A1-A2 product) at Arg³⁷² in the presence of mAb216 was increased ~2-fold compared to control within 15 min, similar to that seen with FXa-catalysed activation in clotting assays. The derived A2 product gradually diminished at 20 min or later in the presence of mAb216, however, and this resulted in a decreased ratio of A2/A1-A2, indicating further proteolysis of FXa within the A2 domain. These findings strongly suggested that mAb216 elevated FVIII activity by accelerating cleavage by thrombin (and FXa) at Arg³⁷².

Effect of mAb216 on FVIII-thrombin interaction

The possibility that the enhancing effect of mAb216 on thrombin-catalysed FVIII activation might be due to the alteration of FVIII-thrombin interaction was further examined using FXa generation assays. Various concentrations of FVIII were incubated with mAb216 (5 μg/ml) and were activated by thrombin (1 nM) prior to the addition of FIXa (0.5 nM) and FX (400 nM) (► Fig. 5). The V_{max} of FXase in the presence of mAb216 was ~1.4-fold greater than that in its absence (127 ± 12 and 89 ± 9 nM/min, respectively), and was similar to that seen in earlier experiments. Notably, the affinity of the interaction between FVIII and thrombin was ~2-fold higher in the presence of mAb216 than in its absence (K_m ; 16.8 ± 2.8 and 33.5 ± 4.2 nM, respectively), suggesting that mAb216 strengthened this interaction and was a consequence of the increased thrombin-catalysed FVIII activation. However, mAb216 preincubated with FVIIIa (thrombin-activated FVIII) did not affect the kinetic parameters for the FIXa-catalysed FX activation on the FXase complex, compared to its absence (V_{max} : 164 ± 18 and 162 ± 16 nM/min and K_m : 8.7 ± 1.6

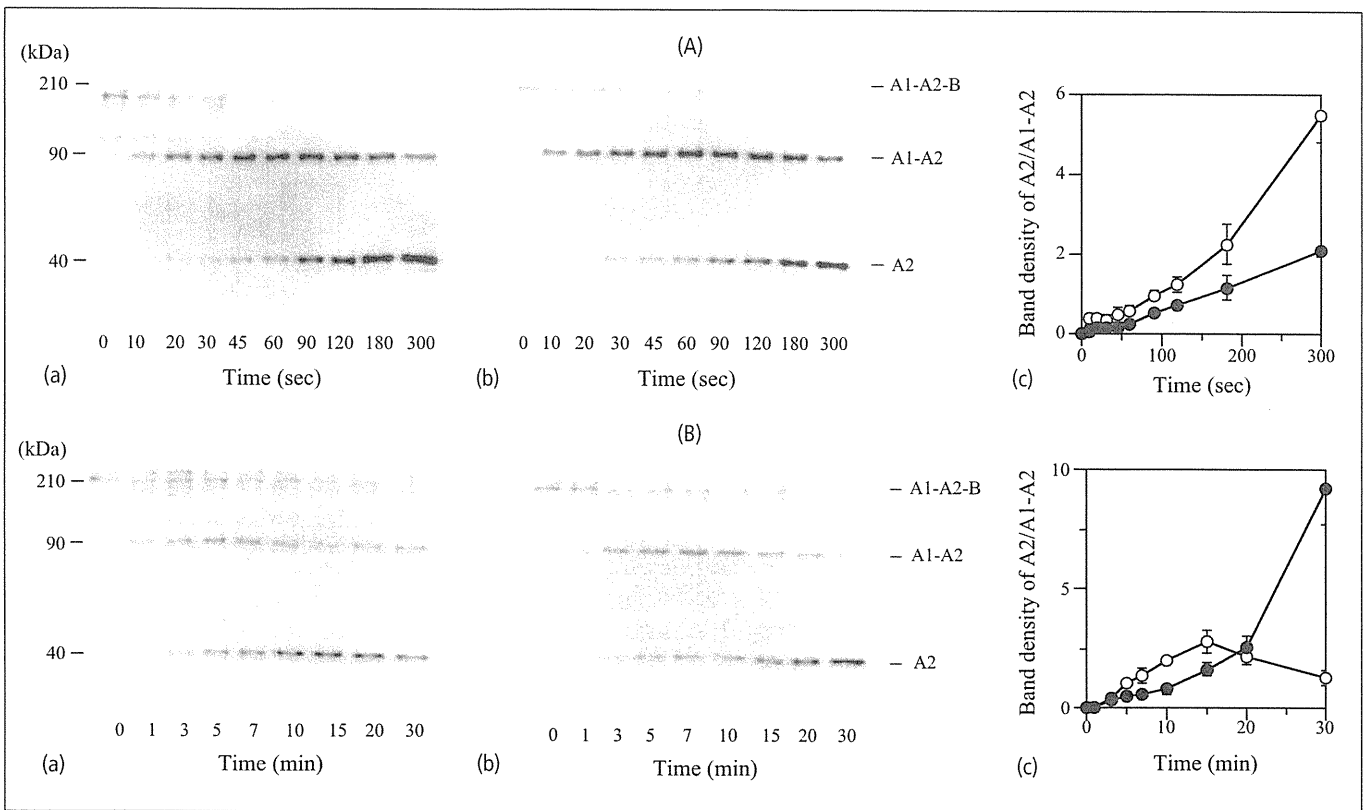


Figure 4: Effects of mAb216 on cleavage of FVIII HCh by thrombin and FXa. FVIII (100 nM) was incubated with thrombin (1 nM, A) or FXa (4 nM, B) plus phospholipid (10 μ M) in the presence of mAb216 (10 μ g/ml, a) or normal IgG (b) for the indicated times. Samples were run on 8% gels followed by Western blotting using biotinylated anti-A2 mAbJR8. Panel c shows quantitative densitometry of the ratio of A2/A1-A2 subunit in the presence of mAb216 (\circ) or normal IgG (\bullet). Experiments were performed three separate times, and the average values and standard deviations are shown.

and 10.7 ± 2.4 nM, respectively) (*inset*). In addition, thrombin generation assay also showed that the presence of mAb216 little affected the effect of adding FVIIIa in FVIII-deficient plasma compared to its absence (data not shown), supportive of no direct effect of this mAb for FVIIIa cofactor function. Taken together, these findings indicated that mAb216 specifically moderated FVIII-thrombin interaction.

Effect of mAb216 on decrease of FVIII activity by anti-FVIII inhibitory antibodies

We further examined whether the FVIII-enhancing effect of mAb216 could be observed even in the presence of anti-FVIII neutralising antibodies. FVIII (4 nM) was incubated with the anti-FVIII inhibitor mAbs, C5 (anti-A1), 413 and JR8 (anti-A2), JR5 (anti-A3), NMC-VIII/5 (anti-C2) or control IgG for 1 h, followed by a further 1-h incubation with mAb216 (2.5 and 5 μ g/ml). The inhibitor titers of the anti-FVIII inhibitor mAbs were adjusted to 3 BU/ml, and FVIII activity was subsequently measured at intervals by one-stage clotting assays. Elevation of FVIII activity with mAb216 alone and initial FVIII activity with anti-FVIII mAbs alone were regarded as 100% and 0%, respectively. The mAb216 enhanced FVIII activity even the presence

of each anti-FVIII inhibitor mAb, and these effects showed the similarity of increase of FVIII activity in the absence of anti-FVIII mAbs (\blacktriangleright Fig. 6). In particular, mAb216 (5 μ g/ml) was required to overcome the inhibitory effects of the anti-FVIII inhibitory mAbs. Similar experiments were repeated using anti-FVIII alloAbs with A2 or C2 epitopes, derived from multi-transfused patients with haemophilia A. The mAb216 was shown to enhance FVIII activity even the presence of these anti-A2 or C2 alloAbs (data not shown). These results supported that even in the case of haemophilia A with inhibitors there was improved function of FVIII when mAb216 is present.

Effect of mAb216 on stability in FVIII and FVIIIa activity

The stability of FVIII or FVIIIa activity likely correlates with intra-subunit interaction within its protein. Ansong and Fay (20) have reported that the temperature-dependent decrease in FVIII activity resulted from the instability for interactions between the HCh and LCh. Hence, to investigate whether mAb216 affected the stability of FVIII activity, we assessed temperature-dependent decreases in FVIII activity. FVIII (1 nM) or normal plasma was pre-

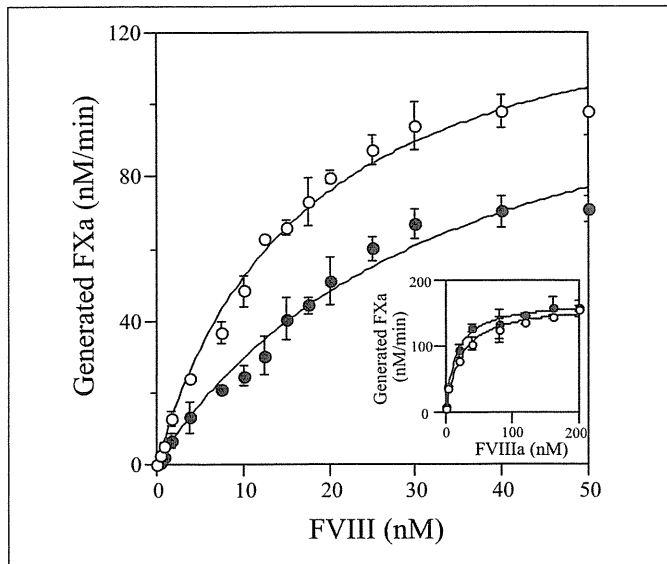


Figure 5: Kinetic analyses of FXase complex in the presence of mAb216. Various concentrations of FVIII were preincubated with mAb216 (5 $\mu\text{g/ml}$, \circ) or normal IgG (\bullet) and were activated by thrombin (1 nM). FXa generation was initiated by adding of FIXa (0.5 nM) and FX (400 nM) as described in *Methods*. *Inset:* Various concentrations of FVIII were activated by thrombin (10 nM) prior to reaction with mAb216 (5 $\mu\text{g/ml}$, \circ) or normal IgG (\bullet). FXa generation was initiated by adding of FIXa (0.5 nM) and FX (400 nM). Data were fitted to the Michaelis-Menten equation. Experiments were performed three separate times, and the average values and standard deviations are shown.

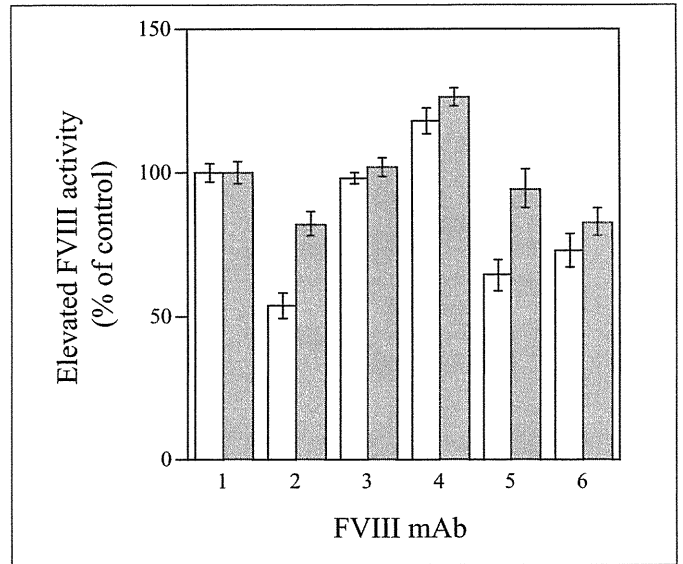


Figure 6: Effect of mAb216 on the decrease of FVIII activity by anti-FVIII mAbs. FVIII (4 nM) was incubated with anti-FVIII mAb (final concentration 3 BU/ml) for 1 hour, followed by a further 1-hour incubation with mAb216 (2.5 $\mu\text{g/ml}$; *white bar*, 5 $\mu\text{g/ml}$; *gray bar*). FVIII activity was measured in one-stage clotting assays. FVIII mAbs 1–6 show normal IgG, anti-A1 (C5), anti-A2 (413), anti-A2 (JR8), anti-A3 (JR5), and anti-C2 (NMC-VIII/5), respectively. Elevation of FVIII activity in the presence of mAb216 alone and initial FVIII activity in the presence of anti-FVIII mAbs alone were regarded as 100% and 0%, respectively. Experiments were performed five separate times, and the average values and standard deviations are shown.

incubated with mAb216 or control IgG before measuring FVIII activity at intervals in mixtures incubated at 55°C (► Fig. 7A). FVIII activity in plasma was more stable (~ 2 -fold) than that of purified FVIII ($t_{1/2}$; 11.5 ± 2.4 and 5.8 ± 1.1 min, respectively), in keeping with the suggestion that VWF protects FVIII. In addition, FVIII activity in both normal plasma ($t_{1/2}$; 20.4 ± 3.1 min) and purified FVIII (12.9 ± 1.7 min), preincubated with mAb216, was significantly more stable (~ 2 -fold) than in the presence of control IgG. Other anti-A2 mAbs (JR8 and 413) did not affect stability (data not shown).

FVIIIa activity is unstable and spontaneously decays. This lability reflects the dissociation of A2 subunit from FVIIIa molecule (21). Therefore, we examined the effect of mAb216 on the stability of FVIIIa activity. FVIII (10 nM) preincubated with mAb216 (10 $\mu\text{g/ml}$) was reacted with thrombin (10 nM) for 1 min to reach maximal FVIII activity, followed by measuring the FVIIIa activity at timed intervals in a one-stage clotting assay (Fig. 7B). The mAb216 ($0.027 \pm 0.002 \text{ min}^{-1}$) prolonged FVIIIa activity by depressing (by ~ 2.5 -fold) the rate of A2 dissociation, compared to normal IgG ($0.066 \pm 0.002 \text{ min}^{-1}$). Taken together, these data demonstrated that mAb216 stabilised both activities of FVIII and FVIIIa.

Discussion

The inhibitory mechanisms of most anti-FVIII antibodies, including alloAbs developed in haemophilia A patients, autoAbs, and mAbs, have been well-analysed (5) and have been shown to decrease or neutralise FVIII activity through direct or indirect inhibitory effects on FVIII function or enhanced clearance of FVIII from circulating blood. Some anti-FVIII antibodies, lacking the ability to inhibit FVIII activity (i.e. non-inhibitory antibodies) have been identified in both normal plasma and haemophilia A patients using ELISA-based assays (22). Most of these non-inhibitory antibodies, however, appear to have little significant function, and relevant epitopes remain to be determined. We anticipated that the range of non-inhibitory antibodies might include immuno-reactants that enhance FVIII activity. In the present report we describe for the first time an anti-FVIII mAb, mAb216, that recognised an A2 epitope and enhanced FVIII activity by ~ 1.5 -fold in plasma-based assays. The antibody also increased the generation of both FXa and thrombin to a similar extent.

Antibodies are known to be versatile molecules that have properties beyond their immunological function, and have been shown to modify the biochemical and biological properties of their target proteins. For example, FVIII antibodies can serve as enzymes with catalytic properties (23). In addition, Kerschbaumer et al. (24) reported a unique anti-FIXa mAb, 224AE3, which enhanced the

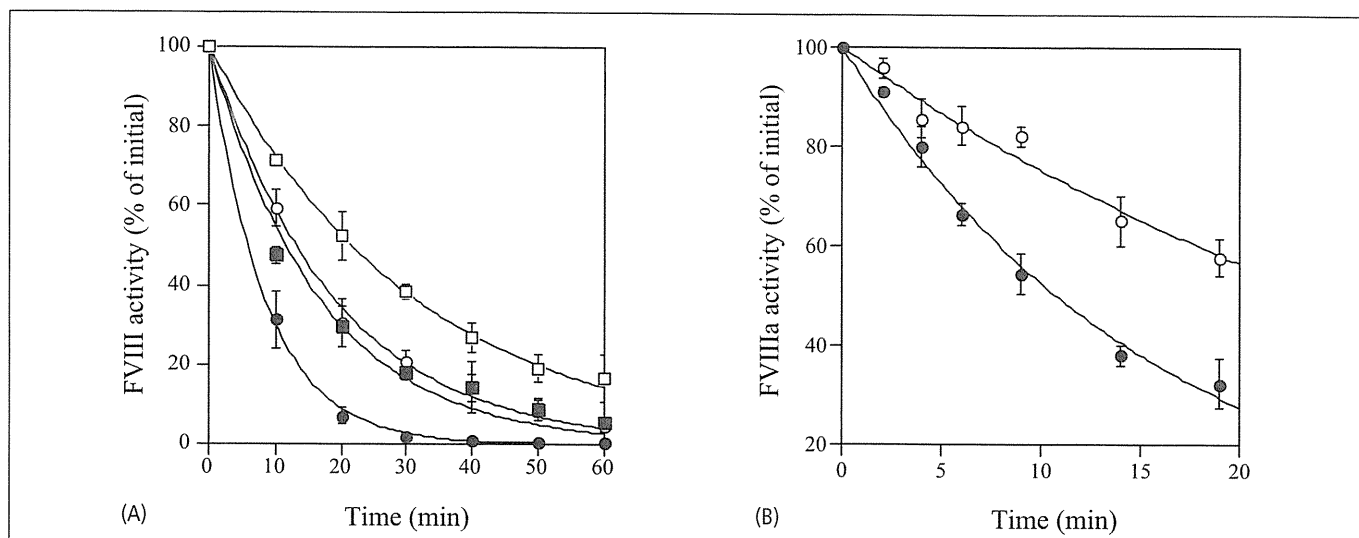


Figure 7: Effects of mAb216 on FVIII and FVIIIa stability. A) FVIII stability: FVIII (1 nM) reacted with mAb216 (10 µg/ml, ○) or normal IgG (●), and normal plasma reacted with mAb216 (10 µg/ml, □) or normal IgG (■), were incubated at 55°C. Aliquots were removed at the indicated times and assayed to determine the FVIII activity. Data were fitted to the formula given in Equation 2. B) FVIIIa stability: FVIII (10 nM) preincubated with mAb216

(10 µg/ml, ○) or normal IgG (●) was activated with thrombin (10 nM) at 1 minute for maximal FVIII activity. Aliquots were removed at the indicated times and assayed to determine the FVIII activity. Maximal FVIII activities were regarded as 100% level. Data were fitted to the exponential decay. Experiments were performed four separate times, and the average values and standard deviations are shown.

catalytic activity of the FXase complex. This enhancing effect appeared to be mediated by two mechanisms; i) the FIXa-mAb224AE3 complex bound to FVIIIa (substrate) with an ~18-fold higher affinity than FIXa alone, ii) the catalytic activity (k_{cat}) of the enzyme complex increased by 2- to ~3-fold whilst the K_m for FX was unaffected. In the present study the FVIII-mAb216 complex bound to thrombin (enzyme) with ~2-fold higher affinity than that of FVIII alone, and the catalytic activity of the antibody complex also was increased by ~1.5-fold. The K_m of FX in the FXase-mAb216 complex was unaffected (data not shown). In addition, mAb216 had no direct effect on FVIIIa cofactor function. These results indicated that the enhancing mechanism of mAb216

was remarkably similar to that of mAb224AE3 described by Kerschbaumer et al. (24).

In our studies the FVIII-enhancing effect of mAb216 was attributed to an alteration in the rate of proteolytic cleavage of HCh by thrombin (and FXa), mediated by a modified affinity in the interaction between FVIII and thrombin. The FVIII A2 domain possesses two independent thrombin-binding regions. One appears to be located within residues 484–509 and is responsible for the cleavage of Arg³⁷² at the A1-A2 junction (25). The other is located within the residues 389–394, and is responsible for the cleavage of Arg⁷⁴⁰ at the A2-B junction (26). In the current investigations, the binding of mAb216 to the A2 domain appeared to change the structural conformation, leading to a tighter interaction with thrombin. Consequently, proteolysis by thrombin (and FXa) of the FVIII molecule complexed with mAb216 was faster than in the absence of antibody. It is of interest that thrombin (and FXa) accelerated the cleavage at Arg³⁷² in FVIII complexed with mAb216 whilst cleavage at Arg⁷⁴⁰ and Arg¹⁶⁸⁹ remained unaffected. Our data provide novel information regarding the enhancing mechanism of a unique anti-FVIII antibody, and suggest that further studies on the precise A2 epitope composition of mAb216 could lead to the development recombinant FVIII mutants with superior FVIII coagulant activity.

Moreover, the FVIII-enhancing properties of mAb216 provide the basis for challenging new replacement therapy in haemophilia A. The antibody enhanced FVIII activity and protected the stability of intrasubunit interactions (HCh-LCh interaction and A1-A2 interaction). It seems possible therefore, that intravenous administration of recombinant FVIII complexed with mAb216 could lead to higher levels of FVIII activity and a prolonged half-life compared with the

What is known about this topic?

- Many reports have identified factor (F)VIII inhibitory antibodies with epitopes located in all subunits of FVIII. However, antibodies that promote FVIII activity do not appear to have been reported.
- We found an anti-A2, FVIII mAb216 that augmented procoagulant activity.

What does this paper add?

- We found an anti-A2, FVIII mAb216 that augmented procoagulant activity. This enhancing effect could be attributed to an increase in thrombin-induced activation of FVIII, mediated by cleavage at Arg372 and a tighter interaction of thrombin with the A2 domain.
- The findings may provide the basis for developing new principles for improving the treatment of haemophilia A patients with and without inhibitors.